ESTABLISHING ENZYME COMPLEXES WITH POLYMER AND DNA SCAFFOLDS TO IMPROVE ENZYME CATALYTIC ACTIVITY AND THERMAL STABILITY

by

XUE WANG

(Under the Direction of Sergiy Minko)

ABSTRACT

Enzymes are natural catalysts that orchestrate metabolic processes in live cells. Because of their high efficiency, selectivity, and biocompatibility, the applications of these catalysts were extended to many industrial and biomedical technologies. The properties of enzymes can be described through stability and catalytic activity. This dissertation aims to develop enzyme complexes with polymer and DNA scaffolds to improve thermal stability and catalytic activity of protein molecules. Elevated temperatures are widely used for many applications to increase process rates and decrease bacterial contaminations. However, most mesophilic enzymes denature at temperatures above 50−60 °C due to the unfolding of protein molecules. A “grafting through” conjugation strategy was designed to improve lysozyme thermal stability by the synthesis of a synthetic polymer−enzyme hybrid, and the conjugates have extended lysozyme half-life up to 9 times at 90°C. The mechanism of thermal stabilization was investigated with the addition of polyethylene glycol (PEG) crowders. The catalytic activity is another significant property of enzymes, which describes the efficiency in degrading substrates. Multi-enzyme complexes usually delivered a synergistic effect with higher catalytic activity compared to single molecules. Cellulosomes are bacterial protein complexes that bind and efficiently degrade

lignocellulosic substrates with synergy effects of different enzymes. Creation of artificial cellulosomes based on DNA scaffolds was developed to illustrate the synergy effect of enzymatic complexes and discover impacts of sequencing and spatial arrangement of enzymes in the complex.

INDEX WORDS: Enzyme Complex, Thermal Stability, Catalytic Activity, Polymer, DNA Scaffold, Cellulosome

# ESTABLISHING ENZYME COMPLEXES WITH POLYMER AND DNA SCAFFOLDS TO IMPROVE ENZYME CATALYTIC ACTIVITY AND THERMAL STABILITY

by

XUE WANG

BE, Beijing University of Chemical Technology, China, 2011

A Dissertation Submitted to the Graduate Faculty of The University of Georgia in Partial Fulfillment of the Requirements for the Degree

DOCTOR OF PHILOSOPHY

ATHENS, GEORGIA

2020

© 2020

Xue Wang

All Rights Reserved

# ESTABLISH ENZYME COMPLEX WITH POLYMER AND DNA SCAFFOLDS TO IMPROVE ENZYME CATALYTIC ACTIVITY AND THERMAL STABILITY

by

XUE WANG

| | |
|---|---|
| Major Professor: | Sergiy Minko |
| Committee: | Vladimir Popik |
| | Jason Locklin |

Electronic Version Approved:

Ron Walcott
Dean of the Graduate School
The University of Georgia
December 2020

# DEDICATION

I dedicate this dissertation to my family. Mom and dad, without your support, I could not realize this journey. Your love always gives me the courage and energy to go through all the difficult times. I am so proud of being your daughter. Chuan, my dear husband, I am so grateful for your caring in life and support and encouragement in my studies. I could not finish this wonderful and challenging journey without your love.

ACKNOWLEDGEMENTS

I would like to thank my family for their support during my Ph.D. study. Chuan, my dear husband, thank you for your caring and encouragement for the past years. I cannot imagine how I would have gotten over the depression without your company. Mom and dad, I am so lucky to be your daughter. You have given me all your love. Thank you for your 24-hour stand-by for my calls and problems, even though we are thousands of miles apart with 12-hour jet lag. I love you.

I would like to thank my PI, Dr. Sergiy Minko, for your endless support and instruction. Thank you for showing me what a real scientist should do and offered me the amazing opportunity to work in BNL. Your guidance and passion for work will inspire me in my future career life. To my committee members, Dr. Popik and Dr. Locklin, thank you for your time, advice, and knowledge to help me better conduct my projects.

Finally, I would like to thank all my collaborators and lab mates. Dmytro, thank you for giving me all the support when I was in BNL. I could not have had a wonderful journey without your help. Nannan, thank you for your close collaboration so we could finish the project smoothly. Thank you, Jacob and Brianna. It was amazing to be your friends and to share times of happiness and depressions with you. Thank Sekhar and Amine for your advice on my research, and thank you, Anu, for your massage. I appreciate having all of you during my incredible Ph.D. journey.

TABLE OF CONTENTS

LIST OF TABLES

LIST OF FIGURES

Page

# CHAPTER 1

# INTRODUCTION AND LITERATURE REVIEW

Enzymes are natural catalysts that orchestrate metabolic processes in live cells. Due to their high efficiency, selectivity, and biocompatibility, the applications of these catalysts were extended to many industrial and biomedical technologies for chemical synthesis, biofuel production, food and cosmetic industries, biosensors, and cloth laundry and decontaminations, to name a few[1-7]. However, the high prices and narrow range of temperature tolerance have limited their practical applications. It is essential to develop enzymes with enhanced catalytic activity and improved thermal stability to be more compatible with industrial requirements.

## Enzyme Thermal Stability

Protein modules are in equilibrium between the folded (N) and unfolded (U) states and strongly favor the folded state at physiological conditions. However, the molecules could shift to the unfolded state at low and high temperatures, pHs, and high concentrations of denaturants[8], and all enzymes will eventually lose catalytic activity with elevated temperature incubation. The overall process can be depicted by the classical scheme of Lumry and Eyring[9]: $N \rightleftarrows U \rightarrow I$, where the native enzyme, N, reversibly unfolded to a denatured state, U, following by irreversible transition to an inactive conformation, I.

The first and universal step of enzyme thermal inactivation is unfolding[10-12]. Under room temperature, the enzyme structure is maintained by hydrogen bonds, hydrophobic, ionic, and van der Waals interactions[13]. The elevated temperature interrupts the noncovalent interactions and

disperses the amino acid residues comprising enzyme active sites, leading to a loss in enzyme activity[14, 15]. With prolonged incubation at high temperature, different subsequent deformations occur in specific types of unfolded enzymes. One is covalent changes, which usually happens among sulfur-containing amino acids. Upon heating, the broken S-S bonds tend to form new intermolecular or intramolecular bridges, which may be different from the original formation, and cause activity loss at alkaline pH[16]. The other is the noncovalent transformation. Thermally unfolded enzymes can undergo polymolecular and monomolecular processes, causing irreversible inactivation of enzymes. Upon unfolding, the hydrophobic portions of enzymes, which were folded into the interior of the structure, were exposed. These hydrophobic interfaces tend to avoid interaction with aqueous solvent and form intermolecular aggregations to reduce the free energy of the system[17]. In dilute solutions, aggregations are limited, however, proteins may intramolecularly refold to stable inactive structure. The incorrect structure cannot be recovered after cooling as a result of high kinetic barrier[18, 19].

Herein, to maintain lysozyme activity at high temperatures, it is significant to explore methods in eliminating the unfolding of protein globules and preventing the formation of incorrect conformations or aggregations. The impact of pH should also be taken into consideration since the thermal behavior of lysozyme is pH related.

**Methods to Improve Enzyme Thermal Stability**

A number of approaches have been proposed to address the challenge of enzyme thermal stability. Among them is the concept of synthetic enzymes or synthetic biology, where the mutated enzyme structure is modified and tuned using genetic tools[20-22]. At the same time, an alternative field of enzyme-synthetic molecule conjugates is shifting the paradigm of synthetic

enzymes by expanding the modification methods with the approaches that either use synthetic polypeptides[23], biomimetic synthetic structures[24] or combine enzyme with synthetic molecules and nanoparticles.[25] In a complex enzyme structure, only 2-3 amino acid residues form the catalytic site. All other amino acid residuals are serving for various functions, including formation and stabilization of the 3D-structure, affinity, and binding to specific substrates, communications with cells, etc. Any modification of the enzyme structure by conjugation with synthetic molecules, regardless of the binding site and size of the conjugate, will result in the synthesis of a new synthetic enzyme with modified properties.

Conjugation of enzymes with polymers has been broadly used to improve shelf-life, immobilize enzymes on solid substrates for heterogeneous catalysis, or for improved *in vivo* delivery of enzymes.[26] In many examples, the polymer-conjugated enzymes have been proven to possess improved stability in a wide range of pH and temperatures[27].

Macromolecular crowding effects on enzyme thermal stability have also been extensively discussed in literature[28-31]. Generally, crowding effects arise from excluded volume effects and soft interactions. Because of the ability of macromolecules to occupy positions in solution, it excludes other molecules from neighborhoods. The addition of macromolecules leads to a less random distribution of molecules in the solution, which results in the decrease of entropy and, consequently, an increase of the particle's free energy[32]. The protein prefers the more compact native state instead of the unfolding denatured due to the limited space[33, 34]. Another impact of the crowding effect is the soft interactions between macromolecules and proteins. Soft interactions can be attractive and repulsive. Repulsive interactions stabilize proteins due to reinforcement of the excluded-volume effect, but attractive destabilizes[35]. The overall crowding effect on enzyme stability is the net effect of excluded volume and chemical interactions.

**Cellulosome – Natural Multi-enzyme Complex with Enhanced Catalytic Activity**

With the growing demand of energy in modern society, the excessive use of fossil fuels, which is responsible for global warming and energy crises, has raised the necessity for innovative and sustainable substitutes for petroleum[36, 37]. Biofuels, such as bioethanol, are proper alternatives, which can be produced from the fermentation of soluble sugars hydrolyzed from lignocellulosic biomass. Lignocellulose, consisting of cellulose, hemicellulose, and lignin, is the most abundant sustainable natural resource of carbohydrate polymer and substrate available for conversion to fuels. However, the process has been limited by the hydrolysis of cellulosic biomass because of its recalcitrance to enzyme hydrolysis[38-40]. The recalcitrance is attributed to the interconnected units in lignocellulose, where lignin and carbohydrates (cellulose and hemicellulose) form lignin-carbohydrate complexes[41]. Besides, the highly crystalline and microfibril structure of cellulose has also put an obstacle to enzymatic digestion of polysaccharides into fermentable sugars[42]. Current conversion processes mainly rely on thermo-chemical pretreatment and high enzyme loading, resulting in high manufacturing costs and expensive final products. Cellulases that possess high catalytic activity can be a potential solution to overcome the economic barriers on biomass conversion.

Cellulosomes are multienzyme complexes either attached to or secreted from cells. The cellulosome from the anaerobic thermophilic bacterium *Clostridium thermocellum* was first identified in the early 1980s and defined as a "discrete, cellulose-binding, multienzyme complex that mediates the degradation of cellulosic substrates" [43, 44]. Cellulosomes contain one noncatalytic protein, named scaffoldin, decorated with multiple cohesins. Catalytic modules with dockerins are assembled to the scaffoldin through cohesin-dockerin interactions. Most scaffoldins also carry one carbohydrate-binding module (CBM) that can anchor the complex to

the cellulose surface[45-48] (Figure 1.1). *C. thermocellum* cellulosome has shown efficient synergism in solubilizing bacterial and *Valonia* cellulose with 75% and 100% crystallinity separately[49], and the activity of cellulosome against crystalline cellulose is 50-fold higher than the corresponding *Tricoderma* free cellulase system[38, 50]. The synergistic interaction can be attributed to the spatial proximity of enzymes grafted and the substrate targeting of CBM[51].

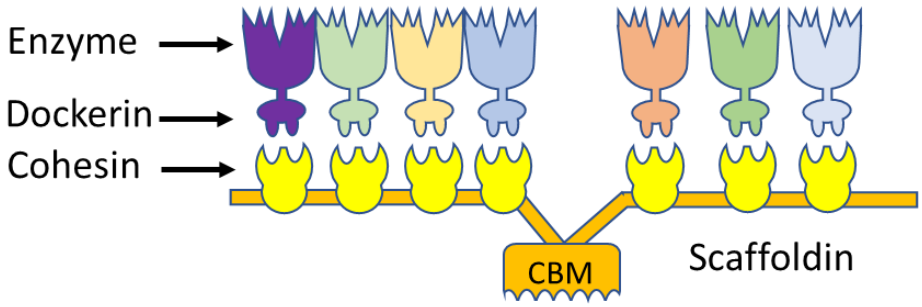


**Figure 1.1** Simplified scheme of a typical cellulosome.

**Creation of Artificial Cellulosomes**

The high efficiency of natural cellulosomes in degrading cellulosic biomass has inspired scientists to develop artificial multienzyme complex to reconstruct the natural structure. The flexibility of building artificial cellulosomes should be more compatible with industrial applications and could help to investigate the mechanism of the cellulosome synergy effect.

The first artificial cellulosome (also called designer cellulosome) was constructed in 2001, where two cellulases from *Clostridium cellulolyticum* (family-5 CelA and family-48 CelF) were anchored onto the chimeric scaffoldin through dockerin-cohesin interaction. The activity of the complex without CBM was enhanced by 1.5-fold comparing to free enzyme mixtures, demonstrating the proximity of enzymes is critical to the synergy effect. The introduction of

CBM further enhanced the activity to 3-fold, indicating the advantage of substrate targeting[52]. The full sequence of cellulosome from *Clostridium thermocellum* was reconstructed *in vitro*, and the reconstituted full-size cellulosome was 21% less active than natural cellulosome[53].

Non-cellulosomal scaffolds have also been developed for cellulases immobilization to improve cellulosome activity and stability. Nanospheres are promising scaffolds according to the high surface area and low diffusion limitation. Cd-Se nanoparticle based cellulosomes were designed through biotin−avidin interaction[54, 55]. The immobilized complex showed enhanced activity in cellulose degradation, and the increase of CBM valency could further enhance enzyme activity. Endoglucanase from *Trichoderma viride* was covalently assembled on polystyrene nanospheres, and the complexes degraded microcrystalline cellulose and cultured wood cells more efficiently than free cellulases according to a higher affinity[56]. To eliminate negative effects from chemical modifications, an endoglucanase CelA and an exoglucanase CelE were conjugated onto CdSe–ZnS core–shell quantum dots (QDs) with two sizes (5nm and 10nm diameter) based on metal affinity coordination without chemical modifications. The complex demonstrated a 2-fold increase of hydrolysis on phosphoric acid-swollen cellulose (PASC), and the proximity of enzymes proved to be more crucial than particle size in activity enhancement[57]. The nanoparticle-based cellulosomes have demonstrated a synergy effect against crystalline cellulose; however, control of the enzyme loading position and the complex composition analysis seems impossible with the above methods.

Though extensive research tried to mimic cellulosome to deliver advanced activity, the behavior of artificial cellulosome is still far away from the natural complex[58]. It is mainly because the mechanism of cellulosome hydrolysis is not fully discovered, such as the impact of

sequence and spatial arrangement of cellulases and CBM. Further understanding is still needed before cellulosomes can fulfill industrial applications.

**Objectives and Dissertation Outline**

The objective of this dissertation are as follows: (1) develop a grafting through method to implant lysozyme into molecular brushes to improve biocatalytic activity and thermal stability; (2) explore the mechanism of polyethylene glycol (PEG) crowding effect on lysozyme thermal stabilization; (3) create artificial cellulosomes with DNA scaffolds and discover the sequencing and spatial arrangement impact on complex synergism.

The rest of the dissertation is organized into five chapters. Chapter 2 reports a "grafting through" conjugation strategy to improve lysozyme catalytic activity and thermal stability by the synthesis of a synthetic polymer−enzyme hybrid. The implantation of a single lysozyme molecule in the molecular brush polymer chain resulted in significant improvement of the thermal stability at 90 °C with a 9-time extension in half-life. The improved enzyme performance is explained by the crowding effect provided by the molecular brush architecture of the synthetic hybrid. This chapter was published in *Macromolecules*, 2018, 51, 5039−5047.

Chapter 3 demonstrates the mechanisms of PEG crowding effects on lysozyme thermal stability. PEG with different molecular weights and concentrations were added into lysozyme solutions. The thermal stability of lysozyme samples were demonstrated in terms of activity and conformations. The stabilization of PEG is a result of the suppression of enzyme aggregation at an elevated temperature according to the formation of LYZ-PEG associates.

Chapter 4 describes the method in developing DNA conjugated cellulases/CBM in preparation for artificial cellulosome establishment. Azide-functionalized cellulases and CBM

were first obtained through coupling between lysine amino acid residuals of the proteins and azido-$PEG_3$-NHS-ester. Protein-$N_3$ were then reacted with dibenzocyclooctyne (DBCO) functionalized DNA (DNA-DBCO) to tether a single-stranded DNA to the proteins over strain-promoted alkyne−azide cycloaddition (SPAAC). The conjugated cellulases/CBM were purified by his-tag purification, and the success of DNA labeling was confirmed by electrophoresis.

Chapter 5 details the design of artificial cellulosomes based on DNA scaffolds to discover the sequencing and spatial impact on cellulose hydrolysis. One exoglucanase, one endoglucanase and one CBM were assembled on DNA templates with three binding sites. Cellulases and CBM were conjugated with different DNA linkers, followed by assembly onto a complementary template at specific locations. The catalytic activities of different combinations were compared against filter paper.

Finally, chapter 6 summarizes the projects discussed in the dissertation, and highlights the future directions of the research.

**References**

1. Ansari, S. A.; Husain, Q., Potential applications of enzymes immobilized on/in nano materials: A review. *Biotechnol Adv* **2012,** *30* (3), 512-23.

2. Ariga, K.; Ji, Q.; Mori, T.; Naito, M.; Yamauchi, Y.; Abe, H.; Hill, J. P., Enzyme nanoarchitectonics: organization and device application. *Chem Soc Rev* **2013,** *42* (15), 6322-45.

3. Es, I.; Vieira, J. D.; Amaral, A. C., Principles, techniques, and applications of biocatalyst immobilization for industrial application. *Appl Microbiol Biotechnol* **2015,** *99* (5), 2065-82.

4. Kirk, O.; Borchert, T. V.; Fuglsang, C. C., Industrial enzyme applications. *Curr Opin Biotechnol* **2002,** *13* (4), 345-51.

5. Min, K.; Yoo, Y. J., Recent progress in nanobiocatalysis for enzyme immobilization and its application. *Biotechnology and Bioprocess Engineering* **2014,** *19* (4), 553-567.

6. Misson, M.; Zhang, H.; Jin, B., Nanobiocatalyst advancements and bioprocessing applications. *J R Soc Interface* **2015,** *12* (102), 20140891.

7. Schmid, A.; Dordick, J. S.; Hauer, B.; Kiener, A.; Wubbolts, M.; Witholt, B., Industrial biocatalysis today and tomorrow. *Nature* **2001,** *409* (6817), 258-68.

8. Yamada, H.; Ueda, T.; Imoto, T., Thermodynamic and kinetic stabilities of hen-egg lysozyme and its chemically modified derivatives: analysis of the transition state of the protein unfolding. *The Journal of Biochemistry* **1993,** *114* (3), 398-403.

9. Lumry, R.; Eyring, H., Conformation changes of proteins. *The Journal of physical chemistry* **1954,** *58* (2), 110-120.

10. Kauzmann, W., Some factors in the interpretation of protein denaturation. In *Advances in protein chemistry*, Elsevier: 1959; Vol. 14, pp 1-63.

11. Lapanje, S., *Physicochemical aspects of protein denaturation*. Wiley: 1978.

12. Tanford, C., Protein denaturation. In *Advances in protein chemistry*, Elsevier: 1968; Vol. 23, pp 121-282.

13. Schulz, G. E.; Schirmer, R. H., *Principles of protein structure*. Springer Science & Business Media: 2013.

14. Anfinsen, C.; Scheraga, H., Experimental and theoretical aspects of protein folding. In *Advances in protein chemistry*, Elsevier: 1975; Vol. 29, pp 205-300.

15. Creighton, T., Proteins in solution. *Proteins* **1983**, 265-333.

16. Steinrauf, L. K.; Dandliker, W. B., A Study of the Reaction of the Disulfide Groups of Bovine Serum Albumin during Heat Denaturation1. *Journal of the American Chemical Society* **1958,** *80* (15), 3833-3835.

17. Ahern, T. J.; Klibanov, A. M., Analysis of processes causing thermal inactivation of enzymes. *Methods of biochemical analysis* **1988**, 91-128.

18. Klibanov, A. M.; Mozhaev, V. V., On the mechanism of irreversible thermoinactivation of enzymes and possibilities for reactivation of "irreversibly" inactivated enzymes. *Biochemical and biophysical research communications* **1978,** *83* (3), 1012-1017.

19. Klibanov, A. M., Stabilization of enzymes against thermal inactivation. *Adv. Appl. Microbiol* **1983,** *29* (1), 28.

20. Arnold, F. H., Directed Evolution: Bringing New Chemistry to Life. *Angew Chem Int Ed Engl* **2018,** *57* (16), 4143-4148.

21. Badenhorst, C. P. S.; Bornscheuer, U. T., Getting Momentum: From Biocatalysis to Advanced Synthetic Biology. *Trends Biochem Sci* **2018,** *43* (3), 180-198.

22. Rothlisberger, D.; Khersonsky, O.; Wollacott, A. M.; Jiang, L.; DeChancie, J.; Betker, J.; Gallaher, J. L.; Althoff, E. A.; Zanghellini, A.; Dym, O.; Albeck, S.; Houk, K. N.; Tawfik, D. S.; Baker, D., Kemp elimination catalysts by computational enzyme design. *Nature* **2008,** *453* (7192), 190-5.

23. Kent, S. B., Total chemical synthesis of proteins. *Chem Soc Rev* **2009,** *38* (2), 338-51.

24. Murakami, Y.; Kikuchi Ji, J. I.; Hisaeda, Y.; Hayashida, O., Artificial Enzymes. *Chem. Rev.* **1996,** *96* (2), 721-758.

25. Harris, J. M.; Chess, R. B., Effect of pegylation on pharmaceuticals. *Nat. Rev. Drug Discov.* **2003,** *2* (3), 214-21.

26. Hwang, E. T.; Gu, M. B., Enzyme stabilization by nano/microsized hybrid materials. *Engineering in Life Sciences* **2013,** *13* (1), 49-61.

27. Gauthier, M. A.; Klok, H.-A., Polymer–protein conjugates: an enzymatic activity perspective. *Polymer Chemistry* **2010,** *1* (9), 1352-1373.

28. Kuznetsova, I. M.; Turoverov, K. K.; Uversky, V. N., What macromolecular crowding can do to a protein. *Int J Mol Sci* **2014,** *15* (12), 23090-140.

29. Ellis, R. J., Macromolecular crowding: an important but neglected aspect of the intracellular environment. *Curr Opin Struct Biol* **2001,** *11* (1), 114-9.

30. Feig, M.; Yu, I.; Wang, P. H.; Nawrocki, G.; Sugita, Y., Crowding in Cellular Environments at an Atomistic Level from Computer Simulations. *J Phys Chem B* **2017,** *121* (34), 8009-8025.

31. Gorensek-Benitez, A. H.; Smith, A. E.; Stadmiller, S. S.; Perez Goncalves, G. M.; Pielak, G. J., Cosolutes, Crowding, and Protein Folding Kinetics. *J Phys Chem B* **2017,** *121* (27), 6527-6537.

32. Ralston, G., Effects of" crowding" in protein solutions. *Journal of chemical education* **1990,** *67* (10), 857.

33. Politou, A.; Temussi, P. A., Revisiting a dogma: the effect of volume exclusion in molecular crowding. *Curr Opin Struct Biol* **2015,** *30*, 1-6.

34. Hong, J.; Gierasch, L. M., Macromolecular Crowding Remodels the Energy Landscape of a Protein by Favoring a More Compact Unfolded State. *Journal of the American Chemical Society* **2010,** *132* (30), 10445-10452.

35. Wang, Y.; Sarkar, M.; Smith, A. E.; Krois, A. S.; Pielak, G. J., Macromolecular crowding and protein stability. *Journal of the American Chemical Society* **2012,** *134* (40), 16614-16618.

36. Ragauskas, A. J.; Williams, C. K.; Davison, B. H.; Britovsek, G.; Cairney, J.; Eckert, C. A.; Frederick, W. J.; Hallett, J. P.; Leak, D. J.; Liotta, C. L., The path forward for biofuels and biomaterials. *science* **2006,** *311* (5760), 484-489.

37. Hill, J.; Polasky, S.; Nelson, E.; Tilman, D.; Huo, H.; Ludwig, L.; Neumann, J.; Zheng, H.; Bonta, D., Climate change and health costs of air emissions from biofuels and gasoline. *Proceedings of the National Academy of Sciences* **2009,** *106* (6), 2077-2082.

38. Demain, A. L.; Newcomb, M.; Wu, J. D., Cellulase, clostridia, and ethanol. *Microbiol. Mol. Biol. Rev.* **2005,** *69* (1), 124-154.

39. Himmel, M. E.; Ding, S.-Y.; Johnson, D. K.; Adney, W. S.; Nimlos, M. R.; Brady, J. W.; Foust, T. D., Biomass recalcitrance: engineering plants and enzymes for biofuels production. *science* **2007,** *315* (5813), 804-807.

40. Artzi, L.; Morag, E.; Barak, Y.; Lamed, R.; Bayer, E. A., Clostridium clariflavum: key cellulosome players are revealed by proteomic analysis. *MBio* **2015,** *6* (3), e00411-15.

41. Pan, X.; Kadla, J. F.; Ehara, K.; Gilkes, N.; Saddler, J. N., Organosolv ethanol lignin from hybrid poplar as a radical scavenger: relationship between lignin structure, extraction conditions, and antioxidant activity. *Journal of agricultural and food chemistry* **2006,** *54* (16), 5806-5813.

42. Yang, B.; Dai, Z.; Ding, S.-Y.; Wyman, C. E., Enzymatic hydrolysis of cellulosic biomass. *Biofuels* **2011,** *2* (4), 421-449.

43. Bayer, E. A.; Kenig, R.; Lamed, R., Adherence of Clostridium thermocellum to cellulose. *Journal of Bacteriology* **1983,** *156* (2), 818-827.

44. Lamed, R.; Setter, E.; Kenig, R.; Bayer, E. In *The cellulosome—a discrete cell surface organelle of Clostridium thermocellum which exhibits separate antigenic, cellulose-binding and various cellulolytic activities*, Biotechnol. Bioeng. Symp, 1983.

45. Bayer, E. A.; Chanzy, H.; Lamed, R.; Shoham, Y., Cellulose, cellulases and cellulosomes. *Current opinion in structural biology* **1998,** *8* (5), 548-557.

46. Shoham, Y.; Lamed, R.; Bayer, E. A., The cellulosome concept as an efficient microbial strategy for the degradation of insoluble polysaccharides. *Trends in microbiology* **1999,** *7* (7), 275-281.

47. Bayer, E. A.; Belaich, J.-P.; Shoham, Y.; Lamed, R., The cellulosomes: multienzyme machines for degradation of plant cell wall polysaccharides. *Annu. Rev. Microbiol.* **2004,** *58*, 521-554.

48. Doi, R. H.; Kosugi, A., Cellulosomes: plant-cell-wall-degrading enzyme complexes. *Nature reviews microbiology* **2004,** *2* (7), 541-551.

49. Boisset, C.; Chanzy, H.; Henrissat, B.; LAMED, R.; SHOHAM, Y.; BAYER, E. A., Digestion of crystalline cellulose substrates by the Clostridium thermocellum cellulosome: structural and morphological aspects. *Biochemical Journal* **1999,** *340* (3), 829-835.

50. Ng, T. K.; Zeikus, J., Comparison of extracellular cellulase activities of Clostridium thermocellum LQRI and Trichoderma reesei QM9414. *Appl. Environ. Microbiol.* **1981,** *42* (2), 231-240.

51. Fierobe, H.-P.; Bayer, E. A.; Tardif, C.; Czjzek, M.; Mechaly, A.; Bélaıch, A.; Lamed, R.; Shoham, Y.; Bélaıch, J.-P., Degradation of cellulose substrates by cellulosome

chimeras Substrate targeting versus proximity of enzyme components. *Journal of Biological Chemistry* **2002,** *277* (51), 49621-49630.

52. Fierobe, H.-P.; Mechaly, A.; Tardif, C.; Belaich, A.; Lamed, R.; Shoham, Y.; Belaich, J.-P.; Bayer, E. A., Design and production of active cellulosome chimeras Selective incorporation of dockerin-containing enzymes into defined functional complexes. *Journal of Biological Chemistry* **2001,** *276* (24), 21257-21261.

53. Krauss, J.; Zverlov, V. V.; Schwarz, W. H., In vitro reconstitution of the complete Clostridium thermocellum cellulosome and synergistic activity on crystalline cellulose. *Appl. Environ. Microbiol.* **2012,** *78* (12), 4301-4307.

54. Nakazawa, H.; Kim, D.-M.; Matsuyama, T.; Ishida, N.; Ikeuchi, A.; Ishigaki, Y.; Kumagai, I.; Umetsu, M., Hybrid nanocellulosome design from cellulase modules on nanoparticles: Synergistic effect of catalytically divergent cellulase modules on cellulose degradation activity. *ACS Catalysis* **2013,** *3* (6), 1342-1348.

55. Kim, D. M.; Umetsu, M.; Takai, K.; Matsuyama, T.; Ishida, N.; Takahashi, H.; Asano, R.; Kumagai, I., Enhancement of cellulolytic enzyme activity by clustering cellulose binding domains on nanoscaffolds. *Small* **2011,** *7* (5), 656-664.

56. Blanchette, C.; Lacayo, C. I.; Fischer, N. O.; Hwang, M.; Thelen, M. P., Enhanced cellulose degradation using cellulase-nanosphere complexes. *PloS one* **2012,** *7* (8).

57. Tsai, S. L.; Park, M.; Chen, W., Size‐modulated synergy of cellulase clustering for enhanced cellulose hydrolysis. *Biotechnology journal* **2013,** *8* (2), 257-261.

58. Moraïs, S.; Morag, E.; Barak, Y.; Goldman, D.; Hadar, Y.; Lamed, R.; Shoham, Y.; Wilson, D. B.; Bayer, E. A., Deconstruction of lignocellulose into soluble sugars by native and designer cellulosomes. *MBio* **2012,** *3* (6), e00508-12.

# CHAPTER 2

# GRAFTING THROUGH METHOD FOR IMPLANTING OF LYSOZYME ENZYME IN MOLECULAR BRUSH FOR IMPROVED BIOCATALYTIC ACTIVITY AND THERMAL STABILITY [1]

[1] Wang, X.; Yadavalli, N. S.; Laradji, A. M.; Minko, S. *Macromolecules* **2018,** *51* (14), 5039-5047. Reprinted here with permission of the publisher.

**Abstract**

We report a "grafting through" conjugation strategy to improve lysozyme catalytic activity and thermal stability by the synthesis of a synthetic polymer-enzyme hybrid. The lysozyme was first conjugated with glycidyl methacrylate via ring opening reaction between epoxy groups and lysine residues of the enzyme to synthesize the enzyme macromonomer. The conjugation was followed by free radical copolymerization of the macromonomer with poly(ethylene glycol) methyl ether acrylate (PEGMEA) (Mn=5000g/mol) and poly(ethylene glycol) methyl ether methacrylate (PEGMEMA) (Mn=500g/mol). We demonstrated that implanting a single lysozyme molecule in the molecular brush polymer chain resulted in a significant improvement of the thermal stability up to 90°C and a 9-time extended half-life for this synthetic enzyme structure. The improved enzyme performance is explained by the crowding effect provided by the molecular brush architecture of the synthetic hybrid.

Keywords: grafting through, protein conjugate, enzyme catalysis, thermal stability

**Introduction**

Enzymes are natural catalysts that orchestrate metabolic processes in live cells. Due to their high efficiency, selectivity, and biocompatibility, the applications of these catalysts were extended to many industrial and biomedical technologies for chemical synthesis, biofuel production, in food and cosmetic industries, biosensors, and cloth laundry and decontaminations, to name a few[1-7]. For many practical applications, elevated temperatures are used to increase rates of the processes and decrease bacterial contaminations[8]. Many such applications will benefit from the improved thermal stability of enzymes. However, most mesophilic enzymes denature at temperatures above 50-60°C due to the unfolding of the protein molecules.[9-11] It is

quite a challenging and significant task to develop thermally stable enzymes for many applications[12, 13].

A number of approaches have been proposed to address the challenge. Among them is the concept of synthetic enzymes or synthetic biology, when the mutated enzyme structure is modified and tuned using genetic tools.[14-16] At the same time, an alternative field of enzyme-synthetic molecule conjugates is shifting the paradigm of synthetic enzymes by expanding the modification methods with the approaches that either uses synthetic polypeptides[17], biomimetic synthetic structures[18] or combine enzyme with synthetic molecules and nanoparticles.[19] In a complex enzyme structure, only 2-3 amino acid residues are forming the catalytic site. All other amino acid residuals are serving for various functions, including formation and stabilization of the 3D-structure, affinity, and binding to specific substrates, communications with cells, etc. Any modification of the enzyme structure by conjugation with synthetic molecules regardless of the binding site and size of the conjugate will result in the synthesis of a new synthetic enzyme with modified properties.

Conjugation of enzymes with polymers has been broadly used to improve shelf-life, immobilize enzymes on solid substrates for heterogeneous catalysis, or for improved *in vivo* delivery of enzymes.[20] In many examples, the polymer-conjugated enzymes have been proven to possess improved stability in a wide range of pH and temperatures[21].

The polymer-enzymes hybrid structures have been approached by different synthetic methods as recently summarized by Pelegri-O'Day *et al.*[22] and Yuanyuan Ju *et al.*[23]. The major strategies for polymer-protein conjugations are “grafting to” and “grafting from” methods. This terminology initially used to classify methods for grafting polymer brushes was adapted for polymer-protein conjugates. The grafting to is the most common method, where functionalized

polymers are coupled with complementary functional groups of proteins (commonly, by using amino- and thiol- functional groups of amino acid residuals) to tether polymer chains to the protein molecule. In the grafting from method, an initiator of chain polymerization is bound to the protein. This conjugate is a macroinitiator. In most cases, controlled radical polymerization initiated by the macroinitiator is used for the polymerization of water-soluble monomers. The third, a less common grafting method is "grafting through".[24] In this grafting method, monomer functional groups (in most cases acrylates) are covalently bound to the material, which is prepared for the modification by the grafting through yielding a macromonomer. The grafting through is a "copolymerization" of monomers and the macromonomer. In an adapted for conjugation of proteins grafting through method, a vinyl monomer is covalently bound to the protein molecule. In the latter case, the protein conjugate is a protein macromonomer and can be copolymerized with various other vinyl monomers.

Each of the conjugation methods has *pros* and *cons*. In the grafting to process, unreacted proteins and polymers remain in the reactive mixture. Separation and purification of the conjugate are difficult. In the grating from process, binding of the initiator and adding some ingredients of controlled radical polymerization (monomers, catalysts, and solvents) may inhibit protein functions. The grafting through method shares the *pros* and *cons* of both methods. It appears that one of the advantages of the grafting through method is related to flexibility in the selection of the polymerization reaction since various initiators and polymerization mechanisms could be compatible with vinyl monomers.

It is noteworthy that in all grafting methods, conjugation of enzymes with polymers, monomers, linkers, and initiators and using organic solvents additives for conjugation reactions may result in inhibition of enzyme activity[25]. There is no universal method for the synthesis of

polymer-enzyme hybrids that could guarantee preservation, boosting, or blocking of protein functional properties. Thus, selection of the conjugation method is based on the experimental testing and finding of appropriate conjugation mechanism for each enzyme and application.

In this work, we use the grafting through method for the synthesis of polymer-protein hybrids of an enzyme, lysozyme (LYZ), using radical polymerization mechanism. We consider the advantage of radical polymerization vs. controlled radical polymerization because availability in the first case of many options of an initiator selection to find an appropriate initiation mechanism less damaging for the enzyme. Another advantage is a very fast growth of polymer chains of the conjugates, which could immediately screen and protect enzyme molecules from destructive reactions with free radicals.

Hen egg-white LYZ is one of many enzymes studied for conjugation with polymers using the grafting to [26] and grafting from[27, 28] methods. However, only some of the publications provided analysis of the catalytic activity of the polymer-enzyme hybrids. LYZ catalytic activity is characterized by two common methods. In both methods, *Micrococcus lysodeikticus* cells are used as a substrate. LYZ hydrolyzes the β-(1-4)-glucosidic linkages between the N-acetylmuramic acid and N-acetyl-D-glucosamine residues in the mucopolysaccharide cell wall. In the first classical turbidity assay, changes in light adsorption by the suspension of lysed cells is monitored at 450 nm wavelength. In the alternative method, the substrate is conjugated with a fluorescent dye. The LYZ catalytic hydrolysis releases unquenched dye, which is detected with a fluorescence spectrometer. Both assays provide very close results for native LYZ.[29]

It was reported that the conjugation of LYZ with polyethylene glycol (PEG) with MM >12 kg/mol resulted in complete loss of LYZ activity. The original activity was restored after cleavage of PEG chains.[30] The activity was monitored using the classical turbidity assay.

Recently, lysozyme-PEG-molecular brush conjugates demonstrated a substantial increase of LYZ activity[31]. In the latter case, the enzyme activity was monitored by fluorescence assay. A random copolymer of di(ethylene glycol) methyl ether methacrylate and 2-(2-pyridyldisulfide) ethyl methacrylate with MM of 50 kg/mol was conjugated with LYZ via thiol–disulfide exchange reaction between the thiol (on 2-iminothiolane modified LYZ) and pyridyl disulfide groups as reported by Xiaotian Ji *et al.*[32]. In the latter case, the conjugate maintained original activity of LYZ as demonstrated with the classical turbidity assay. The same assay test confirmed the retained native catalytic activity of LYZ for LYZ- poly( N-isopropylacrylamide) (PNIPAM) conjugates prepared by the grafting from method.[33] This brief overview shows that catalytic activities of conjugates are very sensitive to the structure of the conjugated polymer, conjugation method and possible side reactions. The results may appear contradictive because sometimes small alternations may affect catalytic properties.

In this work, we extend our recent finding about the substantial stabilizing effect on enzyme stability provided by molecular brush structures.[31, 34] In the previous publication, the lysozyme-polymer hybrids were obtained by the grafting to method. It most demonstrated in many publications that polymer brushes made of hydrophilic polymers or polyelectrolytes create microenvironment favorable of catalytic functions of many enzymes.[35-37] Here, we use the grafting through method for synthesis of lysozyme-polymer molecular brush hybrids and testing their catalytic activity.

## Experimental Section

**Materials**. Lysozyme from chicken egg white, glycidyl methacrylate (GMA), ammonium persulfate (APS) and poly(ethylene glycol) methyl ether methacrylate (PEGMEMA, Mn=500

g/mol) were purchased from Sigma-Aldrich. Poly(ethylene glycol) methyl ether acrylate (PEGMEA, Mn=5000 g/mol) was purchased from VWR. An EnzChek fluorescence-based lysozyme assay kit (Catalog No. E22013) was purchased from the Thermo Fischer Scientific.

**GMA conjugate with lysozyme.** Three GMA to lysozyme molar ratios (500:1, 1000:1, 2000:1) were used to find the optimum condition of GMA-LYZ conjugation. A series of reactions mixtures with different LYZ:GMA ratios was prepared by mixing 2.5 mg of LYZ and 11.92, 23.84, or 47.68µL of GMA in 2.5ml phosphate-buffered saline (PBS). The conjugation reaction was conducted overnight at room temperature. The separation of the GMA conjugated lysozyme (GMA-LYZ) from the free GMA was conducted using desalting columns (GE Healthcare 17-0851-01). The conjugates were characterized by a liquid chromatography-mass spectrometry (LC-MS). BioBasic™ 4 LC columns by Thermo Hypersil-Keystone were used with 1mm diameter and 150mm length. The particle size and pore size were 5µm and 300Å. Elution of the analysis was a mixture of 0.05% Trifluoroacetic acid (TFA) in water and actonitrile. Actonitrile concentration was increased from 5% to 100% for the first 25 minutes, then held at 100% for the rest of the run. The MS instrument was Esquire 3000 Plus ion trap by Bruker Daltonics. The average number of GMA per LYZ was calculated by integrating all peaks obtained by LC-MS.

**Polymerization.** The LYZ-polymer conjugates **(**LPCs) were synthesized using free radical polymerization. PEGMEMA and PEGMEA were purified using a flash chromatography column containing inhibitor removers (Sigma #311332). 2.2 mg APS was dissolved in 1ml PBS. Five different PEGMEMA:PEGMEA molar ratio combinations (PEGMEMA only, 6:1, 3:1, 1:1, PEGMEA only) were used to synthesize LPCs. 2 ml of a GMA-LYZ mixture, 200 µL of an APS solution (0.3mM), and one of the PEGMEMA:PEGMEA blends (46.30µl:0g, 39.68µl:0.07g,

34.72µl:0.13g, 23.15µl:0.25g, and 0µl:0.50g) were added to 6.5ml of PBS. The reaction mixture was deoxygenated by running three freeze-pump-thaw cycles, then heated at 50°C for 20 minutes under argon atmosphere. The reaction was terminated by opening the flask to ambient atmosphere and cooling. Molecular mass of the conjugate was measured using gel permeation chromatography (GPC). Copolymer compositions were analyzed with 500Hz nuclear magnetic resonance (NMR).

**LYZ and LPC activity and thermal stability measurement.** LYZ and LPC solutions were preincubated at 90°C for 1 h and cooled to room temperature. These solutions were then mixed with the fluorescein dye-labeled M. lysodiekticus cell wall material (EnzChek lysozyme assay kit) and assayed with a fluorimeter using a 96-well plate reader at 45 °C for 1 h with 2 min intervals. The preincubation was conducted in citrate buffer (pH=5.2) to avoid disulfide bond scrambling within the protein molecule at high temperature. The assay's pH was maintained at 7.4. Fluorescence was measured using a CytoFluor 4000 series fluorescence microplate reader with built-in standard fluorescein filters. The digestion products of the substrate have an absorption maximum at ~494 nm and a fluorescence emission maximum at ~518 nm. The fluorescence was measured using excitation/emission at ~485/530 nm.

**Biocatalytic kinetics for LYZ and LPCs.** The calibration curve of the fluorescein dye was used to estimate the conversion of the substrate and thereby the kinetic parameters of the Michaelis−Menten model for both LYZ and LPCs[31]. In our study, we have employed a *M. lysodeikticus* cell walls substrate concentration ranges from 50 µg/mL to 500 µg/mL, which corresponds to fluorescein concentrations of 0.01−0.1 µM. The study was conducted at 45°C.

## Results

The schematic presentation of the synthetic steps is shown in Figure 2.1. The LPC hybrids were synthesized in two steps. Initially, LYZ was conjugated with GMA to form a LYZ-macromonomer. Then, the macromonomer was copolymerized with two acrylate monomers with side PEG groups PEGMEMA (Mn 500 g/mol) and PEGMEA (Mn 5000 g/mol). Two acrylates with different lengths of PEG side groups were used to regulate stiffness of the molecular brush. The structure of the synthesized LPC is schematically presented in Figure 2.1c.

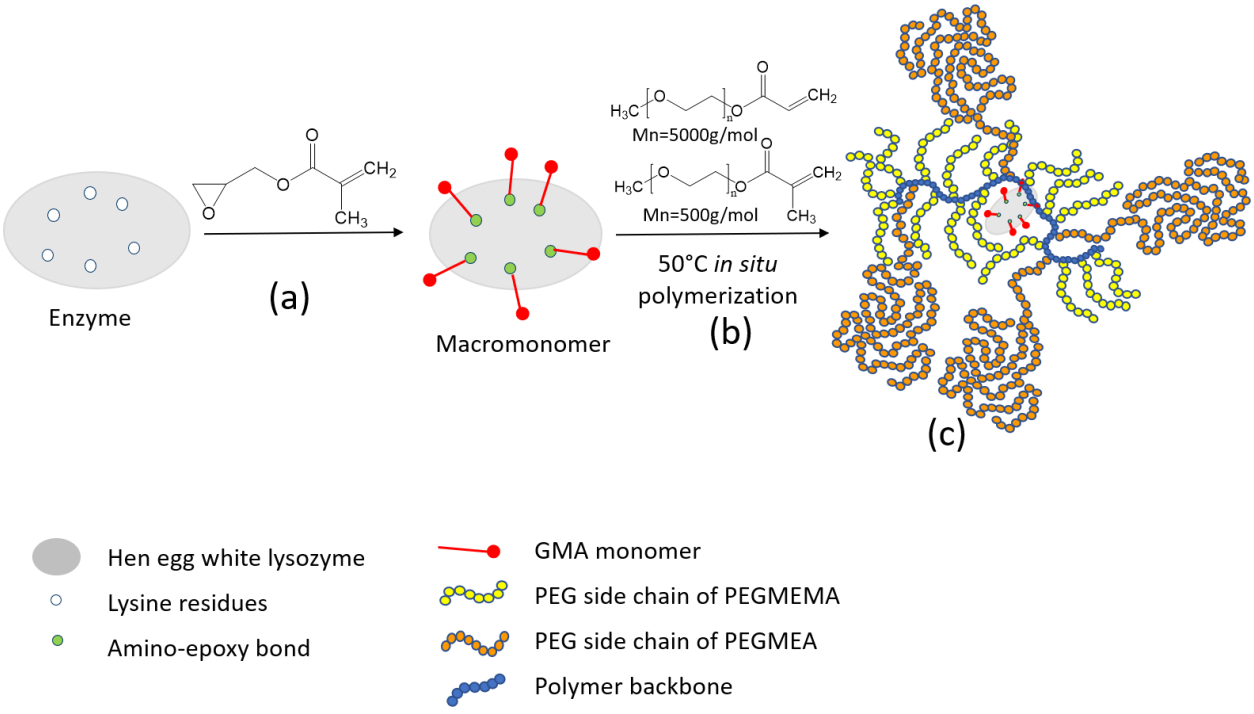


**Figure 2.1** Schematic of the synthesis of the LPC hybrid in two steps: (a) synthesis of the macromonomer using lysine residues of LYZ, (b) copolymerization of the macromonomer with PEGMEA and PEGMEMA, and (c) structure of the molecular brush with implanted LYZ.

**GMA conjugated lysozyme.** The conjugation of LYZ and GMA benefited from the high reactivity of 6 amino groups of lysine residues on the surface of LYZ globule in reaction with

epoxy functional groups of GMA. The LC-MS spectra demonstrated the conjugation efficiencies for three different GMA to LYZ ratios (Figure. 2.2). At most in average four GMA monomers were conjugated with the enzyme at GMA: LYZ molar ratio 500:1, while at GMA: LYZ 1000:1 and 2000:1 ratios, up to 5 to 11 and 7 to 11 GMA molecules respectively were bound to LYZ. Such a high loading of LYZ with GMA could be explained by the attachment of the second GMA molecule to the lysine amino groups.[38] Thus, at the higher aspect ratios the majority of lysine functionalities were involved in the conjugation. The LC-MS spectra revealed no presence of native LYZ after the conjugation reaction (Figure. 2.2c).

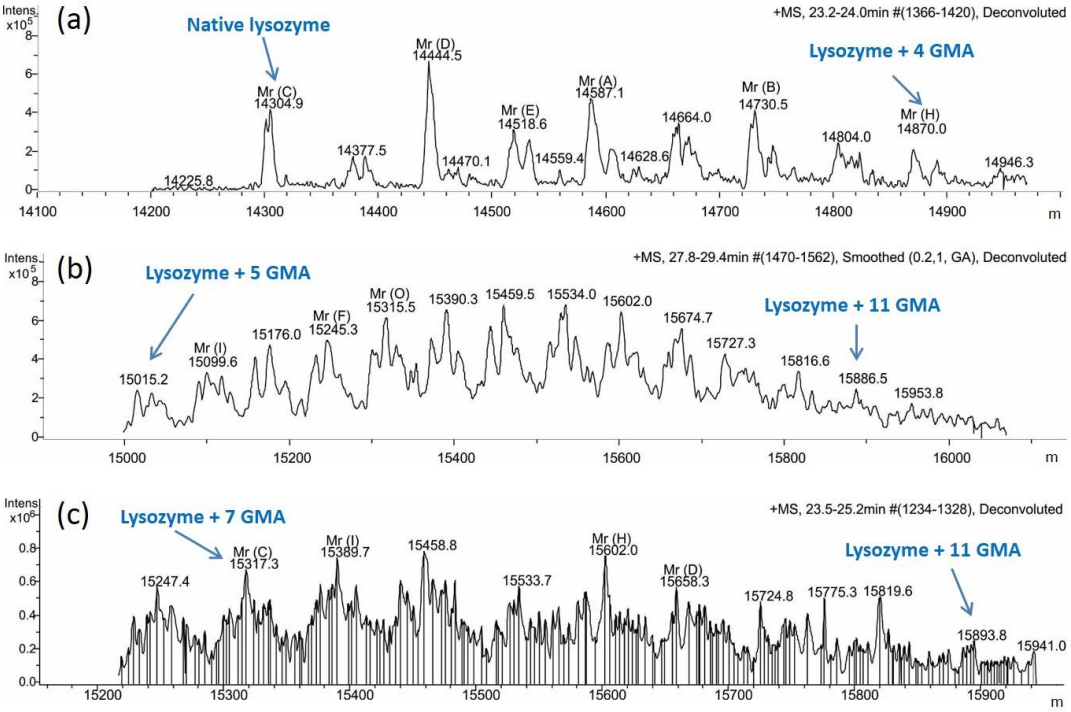


**Figure 2.2** LC-MS spectra of GMA-LYZ conjugates at different GMA: LYZ molar ratios in the reaction mixture: (a) 500:1, the number of GMA residues per LYZ (GMA:LYZ ratio) molecules varies from 0 to 4; in average (GMA:LYZ average) 2 conjugated GMA per LYZ; (b) 1000:1, GMA:LYZ ratio from 5 to 11; GMA:LYZ average = 8; (c) 2000:1, GMA:LYZ ratio from 7 to 11; GMA:LYZ average =8.

In the polymerization experiments, we used GMA-LYZ conjugates prepared at a GMA: LYZ ratio of 1000:1 with an average number of GMA fragments per LYZ molecule of 8. It is obvious, that binding of LYZ to GMA will affect the reactivity of the acrylate monomer because of a steric hindrance. Once one conjugated acrylate monomer is involved in the polymerization, the probability of involvement of other GMA units drops substantially because of a steric hindrance caused by the grafted polymer chain. Thus, the probability of anchoring of GMA-LYZ by more than one GMA residues is very low. However, we selected a macromonomer with 8 GMA units to increase the reactivity (probability free radical-vinyl group collision) of the macromonomer in free radical copolymerization reaction.

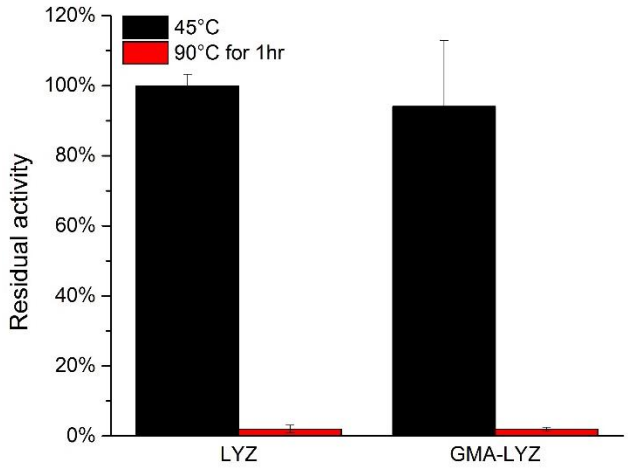


**Figure 2.3** Biocatalytic activity of LYZ and GMA-LYZ after a 1 h incubation time at 45°C (black bars) and 90°C (red bars).

It is well documented that conjugation of enzymes with low and high molecular mass molecules or adding various reactive species to enzyme solutions may impact catalytic functions of the enzyme. In the following experiments, we verified the impact of conjugations and the reagents used in the polymerization reactions on the biocatalytic activity of GMA-LYZ conjugates.

Biocatalytic activity was evaluated with a lysozyme fluorescence assay kit. The activity is shown in percentage referred to 100% activity of LYZ. The effect of GMA was examined by comparing biocatalytic activities of LYZ and GMA-LYZ at 45°C and 90°C following a 1 h incubation. GMA-LYZ and native LYZ demonstrated similar performance at both temperatures indicating no impact of the GMA conjugation on lysozyme (Figure 2.3).

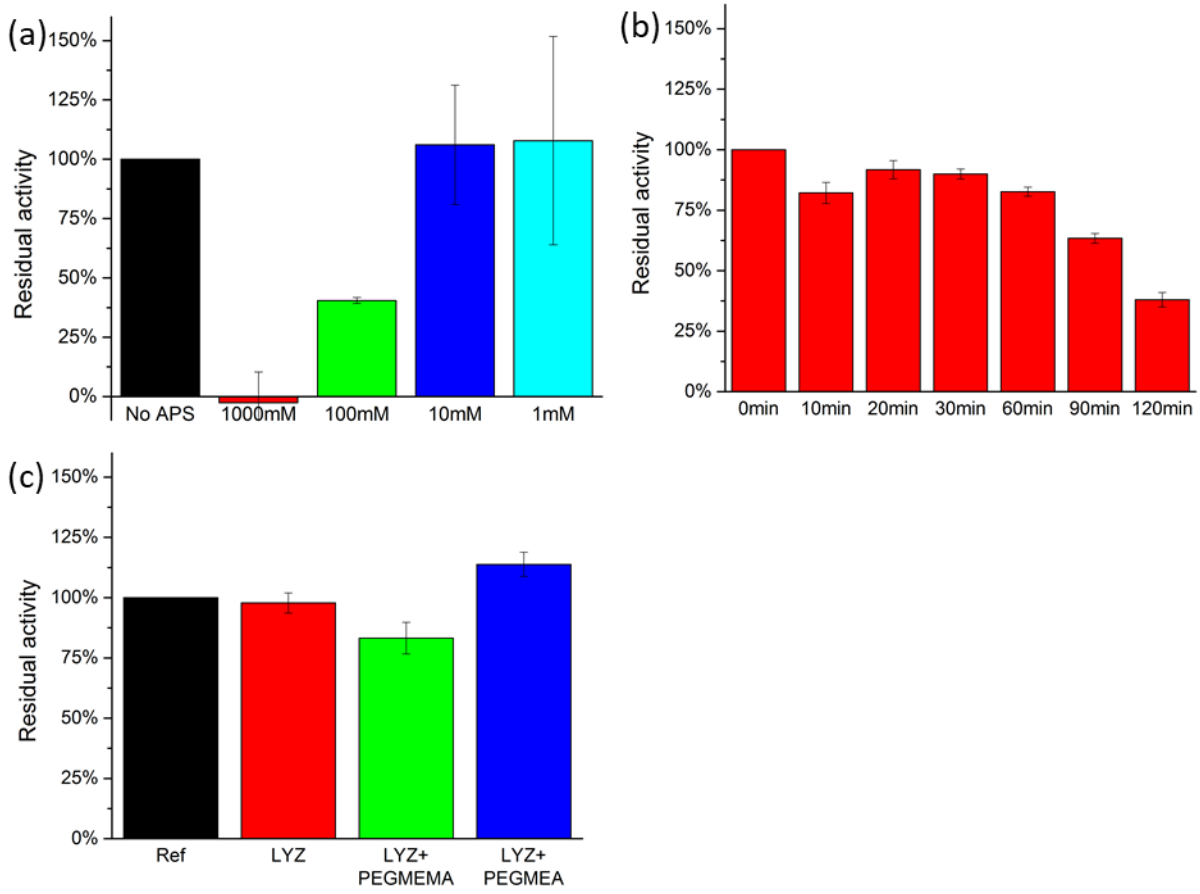


**Figure 2.4** Biocatalytic activity of LYZ in the presence of APS initiator of radical polymerization and acrylate comonomers referred to the activity of native LYZ (Ref) in PBS: (a) the effect of APS concentration at room temperature; (b) the effect of 0.3mM APS incubated at 50°C with different reaction times; (c) the effect of PEGMEMA and PEGMEA monomers incubated at 50°C for 20 min.

**Impact of APS and monomers.** Effects of the APS initiator and monomers on LYZ catalytic activity were examined in reference experiments to select proper polymerization conditions (Figure 2.4). The effect of the APS initiator was studied with no acrylate monomers in the solution. The tests were conducted at different APS concentrations at room temperature and different incubation times at 50°C. The presence of APS results in a loss of catalytic activity of the enzyme at high APS concentrations at room temperature (Figure 2.4a) and a long reaction time at 50°C (Figure 2.4b), however the effect is minimized at lower APS concentrations and becomes negligible at 0.3mM APS if the incubation time is less than 60 min. The time-dependent loss of activity at the elevated temperature provides evidence that free radical affected degradation in the presence of APS. Our following polymerization experiments were conducted at 0.3mM APS for less than 20 min to avoid damaging effect of free radicals.

The effect of acrylate monomers on LYZ activity in the absence of the initiator was tested in another series of reference experiments. Mixing of LYZ with PEGMEMA and PEGMEA monomers had no obvious effects on LYZ biocatalytic activity as could be concluded from the data in Figure 2.4c.

**Synthesis of LPC.** The LPC conjugates were synthesized in a reactive mixture of the GMA-LYZ conjugate macromonomer, PEGMEMA and PEGMEA monomers, APS initiator and PBS using free radical copolymerization mechanism. The composition of the reaction mixtures and synthesized conjugates are shown in Table 2.1 (where, S is the polymerization conversion, PDI is the polydispersity index). The purification and composition analysis of conjugates are presented in detail in Figure A1 and B1.

In the copolymerization, we used small concentrations of GMA-LYZ to synthesize hybrids that contain just one molecule of LYZ per polymer chain. We targeted such a composition of the hybrid that could avoid multiple enzymes per the conjugate and thus possible cross-interactions and cross-linking effects. The polymerization was terminated at conversions below 10%. We did not separate the copolymer with implanted LYZ from that with no enzyme since the latter copolymer is catalytically inert and did not affect the biocatalytic assay.

**Table 2.1** Composition and molecular mass of LPC

| Sample | Monomer mixture, % mol | | | LPC, % mol | | | LYZ per LPC, mol/mol | LYZ, % w | S, % | $M_n$, kg/mol | PDI |
|---|---|---|---|---|---|---|---|---|---|---|---|
| | GMA-LYZ | PEG-MEMA | PEG-MEA | GMA-LYZ | PEG-MEMA | PEG MEA | | | | | |
| LPC 500 | 0.1 | 99.9 | 0 | 0.1 | 99.9 | 0 | 0.09 | 14.6 | 13.8 | 43.3 | 2.71 |
| LPC 6:1 | 0.1 | 85.6 | 14.3 | 0.1 | 90.4 | 9.5 | 0.14 | 8.0 | 6.9 | 116.9 | 1.96 |
| LPC 1:1 | 0.1 | 49.9 | 49.9 | 0.1 | 47.3 | 52.6 | 0.047 | 8.8 | 9.8 | 123.4 | 1.59 |
| LPC 5000 | 0.1 | 0 | 99.9 | 0.2 | 0 | 99.8 | 0.031 | 9.1 | 4.3 | 74.3 | 1.54 |

**Improved thermal stability and half-life of LPCs.** Thermal stability of LPCs was evaluated after incubation in aqueous solution at 90°C. Native LYZ was almost completely denatured when incubated at 90°C for 1 h, while all LPCs retained more than 50% residual activity. Among different LPCs, PEGMEMA only (LPC 500) and PEGMEMA:PEGMEA=6:1 (LPC 6:1) demonstrated lower thermal stability than other conjugates LPC 3:1, LPC 1:1 and LPC 5000 (Figure 2.5). The results of half-life measurements demonstrated the improvement of thermal stability for LPCs. Notably, LPC 1:1 had extended the half-life of the conjugate up to 9

times as compared with that for native LYZ (Figure 2.6). Conjugates with higher contents of PEGMEA showed higher stabilizing effect.

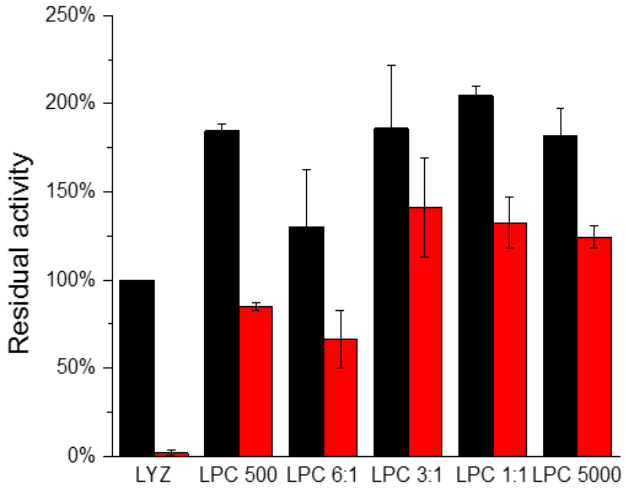


**Figure 2.5** Catalytic activity of LPCs at 45°C (black bars) and incubated for 1 h at 90°C (red bars).

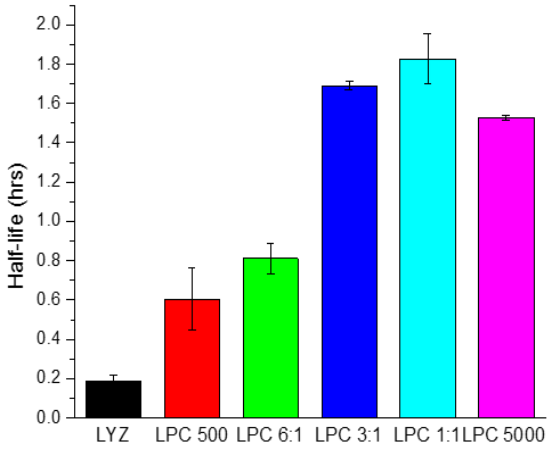


**Figure 2.6** Half-life of native LYZ and LPCs at 90°C

Michaelis−Menten model was used to analyze biocatalytic kinetics for the native LYZ and LPCs (Figure 2.7). LPC 6:1 had similar kinetic constants as native LYZ at 45°C, however, $V_{max}$ was doubled for LPC 1:1 and LPC 5000 (Table 2.2). A greater turnover number ($k_{cat}$) and specificity constant ($k_{cat}/K_M$) of LPC 1:1 and LPC 5000 indicated a higher biocatalytic activity of

the conjugates. The kinetic studies confirmed that after 1 h incubation at 90°C, native LYZ was denatured, while all LPCs remained active yet.

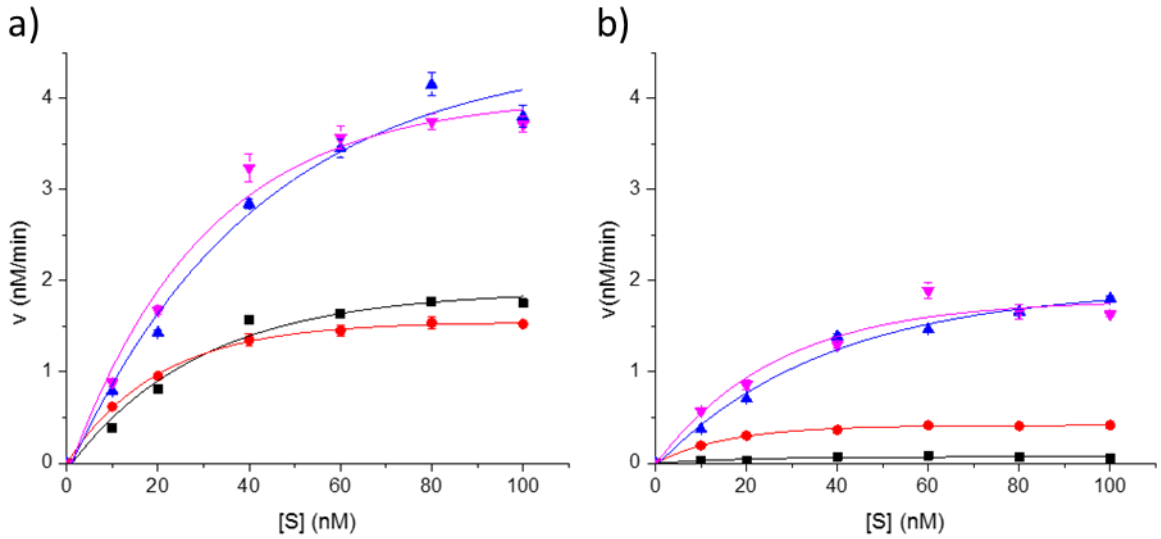


**Figure 2.7** Michaelis-Menten curves for native LYZ, LPC 6:1, LPC 1:1 and LPC 5000 incubated for 1 h at (a)45°C and (b) 90°C.

**Table 2.2** Kinetic constants for LYZ and LPCs at 45°C and after 1-hour incubation at 90°C

| Sample | 45°C | | | | 1 h incubation at 90°C | | | |
|---|---|---|---|---|---|---|---|---|
| | $V_{max}$ (nM/min) | $K_M$ (nM) | $k_{cat}$ ($\times 10^{-5}$ $s^{-1}$) | $k_{cat}/K_M$ ($\times 10^3$ $M^{-1}$ $s^{-1}$) | $V_{max}$ (nM/min) | $K_M$ (nM) | $k_{cat}$ ($\times 10^{-5}$ $s^{-1}$) | $k_{cat}/K_M$ ($\times 10^3$ $M^{-1}$ $s^{-1}$) |
| LYZ | 1.9 ± 0.1 | 21.2 ± 0.9 | 9.8 | 4.6 | - | - | - | - |
| LPC 6:1 | 1.5 ± 0.0 | 16.4 ± 0.3 | 8.1 | 4.9 | 0.4 ± 0.0 | 11.2 ± 0.4 | 2.2 | 1.9 |
| LPC 1:1 | 4.5 ± 0.5 | 30.1 ± 0.9 | 23.5 | 7.8 | 1.9 ± 0.1 | 27.0 ± 0.9 | 10.0 | 3.7 |
| LPC 5000 | 4.0 ± 0.3 | 21.7 ± 0.8 | 20.9 | 9.7 | 1.8 ± 0.2 | 18.7 ± 0.9 | 9.3 | 5.0 |

"-" Indicates no activity detected

**Discussion**

The catalytic activity tests demonstrate that implanting of a single enzyme molecule per a polymer chain with bulky side groups using the grafting through polymerization mechanism results in a quite substantial improvement of both catalytic activity at ambient conditions and thermal stability of the synthetic hybrids at elevated temperatures. This result is in accord with those for the grafting to synthesis of LPC hybrids using molecular brush architecture.[31] The possible explanation of the improved enzyme performance is the effect termed "crowding effect."

The role of the crowding effect on the enzyme stability has been extensively discussed in literature[39-42]. Generally, the crowding effect leads to improved stability of proteins[43] that was confirmed by changes of both unfolding free energy and unfolding kinetics.[44] However, there is no yet clear understanding of specific mechanisms of the stabilization that are likely different for different polymers and proteins.[45-48] PEG is the most studied polymer for the crowding effect when the conjugation of PEG and proteins could have both positive and negative effects on enzyme performance.[49-54] Specifically, the PEG crowding effect for LYZ was recently discussed elsewhere.[34] It was shown that PEG chains concentrated around the enzyme molecules restrict water access and promote the structural stability of LYZ. Stiffness of the molecular brush is a quantitative characteristic that scales with the compression (crowding) of the implanted enzyme molecule.

**Table 2.3** Molecular characteristics of the molecular brush conjugates

| Sample | Distance between side PEG chains, $h$ (nm) | Number average degree of polymerization of side chain, $N_{SC}$ | Brush thickness in melt[55], $R_{SC}$ (nm) | Brush thickness in θ- solvent[56], $R_{SC}$ (nm) | The free energy per chain in the brush in θ- solvent[56], F(h) /$k_BT$ |
|---|---|---|---|---|---|
| LPC 500 | 0.25 | 8.95 | 1.56 | 1.7 | 2.74 |
| LPC 5000 | 0.25 | 111.5 | 5.16 | 9.2 | 6.36 |

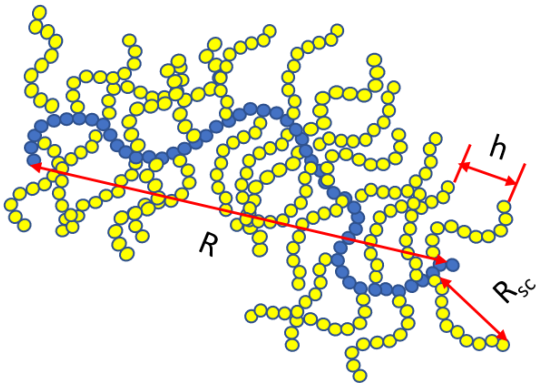


**Figure 2.8** Molecular structure of the bottle-brush architecture

The crowding effect originates from the molecular structure of the bottle-brush architecture (Figure 2.8.). In this work, homopolymer molecular brushes LPC 500 and LPC5000 are made of monomer with the number average degree of polymerization of PEG side groups 8.95 and 111.5, respectively. All other samples are random copolymer of these two monomers. In the latter case, quantitative evaluation of the molecular characteristic of the brush is complicated. We made theoretical analysis of the crowding effect just for LPC 500 and LPC 5000 molecular brushes assuming that copolymers' molecular characteristics and thus the crowding effect fall in the range between these two polymeric structures.

The estimates of molecular dimensions using the scaling theory of the molecular brush in θ-solvent[56] and melt [55] for LPC 500 and LPC 5000 are shown in Table 2.3 (see for details, Table B1 and Table B2). For these two homopolymer molecular brushes, the distance between side PEG group is much smaller than the Gaussian dimensions of PEG side chains. Thus, the side PEG chains and the main backbone of the polymer are extended. Water is a good solvent for PEG. Hence, the extension is much stronger in aqueous solutions than in melt or θ-solvent[56] due to the excluded volume effect. The other studied copolymer molecular brushes made of a

mixture of PEG-acrylates with different sizes of PEG side chains, however, will have a stratified structure of the extended side chains as it is shown in Figure 1c. We may neglect the perturbations induced by the implantation of a single LYZ molecule per one chain in the molecular brush. However, we should consider the pressure experienced by the enzyme owing to the extension of both PEGMEA and PEGMEMA side PEG chains because the LYZ dimensions (about 2 nm) is comparable with the dimensions of short PEG chains in PEGMEMA (Table 2.3). The stiffness of the molecular brush, which is proportional to the brush thickness $R_{sc}$, is indeed greater for LPC5000 than for LPC 500 as obtained from both the theoretical models (Table 2.3). Thus, we could consider that the molecular stiffness of the copolymers will increase with the fraction of PEGMEA.

The crowding effect in the conjugate is directly correlated with brush stiffness and free energy per chain in the brush. The latter was evaluated using the self-consistent field theory model for θ- solvent[56] (Table 2.3). It is obvious from the free energy estimates that the crowding effect much stronger for LPC 5000 brushes as compared to LPC 500 brushes.

This assumption correlates with LPC half-life at 90°C (Figure 2.6) which increases with the increase of a PEGMEA fraction in the copolymers and levels off at its highest content. Both the theoretical models show that the thickness of LPC 5000 brushes is much greater than the LYZ dimensions. The latter could explain some decrease of catalytic activity of LPC 5000 as compared with LPC 1:1 (Figure 2.5 and Table 2.2). The LPCs in a dry state where visualized using scanning probe microscopy (SPM). The single molecule appears in the SPM images as 5-10 nm particles in accord with the theoretically estimated molecular dimensions (Figure B2).

The kinetic constants (Table 2.2) demonstrate that not only thermal stability but also catalytic activity of LPCs is improved. This result indicates that the crowding effect is beneficial

for LYZ performance, specifically for the maintaining of the conformation of the catalytic cavity.

## Conclusion

Here, we reported experimental evidences for substantial improvement of biocatalytic activity and thermal stability of the LYZ-polymer molecular hybrids. The structure of molecular brush and its stiffening mechanism provide quite efficient tools for improvement of the enzyme performance. We consider these hybrid molecules as a type of synthetic enzymes – implanted or grafted enzyme - because the confinement of the enzyme in the molecular brush results in the modification of enzyme properties, specifically a 9-fold longer half-life of the implanted vs. native LYZ at 90°C and higher catalytic activity at ambient conditions. The properties of the polymer-enzyme hybrids can be tuned by the molecular brush composition. It is obvious, that the crowding effect is a very general approach to the modification of enzyme properties. However, it is to discover yet the mechanisms of catalytic site and the entire enzyme globule structural response to the excluded volume effect in the molecular brush structures. The phenomena seem to be quite complex if we consider a shift of the balance of intermolecular interactions of PEG in water with changes of temperature.

## References

1. Ansari, S. A.; Husain, Q., Potential applications of enzymes immobilized on/in nano materials: A review. *Biotechnol Adv* **2012,** *30* (3), 512-23.

2. Ariga, K.; Ji, Q.; Mori, T.; Naito, M.; Yamauchi, Y.; Abe, H.; Hill, J. P., Enzyme nanoarchitectonics: organization and device application. *Chem Soc Rev* **2013,** *42* (15), 6322-45.

3. Es, I.; Vieira, J. D.; Amaral, A. C., Principles, techniques, and applications of biocatalyst immobilization for industrial application. *Appl Microbiol Biotechnol* **2015,** *99* (5), 2065-82.

4. Kirk, O.; Borchert, T. V.; Fuglsang, C. C., Industrial enzyme applications. *Curr Opin Biotechnol* **2002,** *13* (4), 345-51.

5. Min, K.; Yoo, Y. J., Recent progress in nanobiocatalysis for enzyme immobilization and its application. *Biotechnology and Bioprocess Engineering* **2014,** *19* (4), 553-567.

6. Misson, M.; Zhang, H.; Jin, B., Nanobiocatalyst advancements and bioprocessing applications. *J R Soc Interface* **2015,** *12* (102), 20140891.

7. Schmid, A.; Dordick, J. S.; Hauer, B.; Kiener, A.; Wubbolts, M.; Witholt, B., Industrial biocatalysis today and tomorrow. *Nature* **2001,** *409* (6817), 258-68.

8. Iyer, P. V.; Ananthanarayan, L., Enzyme stability and stabilization—Aqueous and non-aqueous environment. *Process Biochemistry* **2008,** *43* (10), 1019-1032.

9. Arakawa, T.; Prestrelski, S. J.; Kenney, W. C.; Carpenter, J. F., Factors Affecting Short-Term and Long-Term Stabilities of Proteins. *Advanced Drug Delivery Reviews* **1993,** *10* (1), 1-28.

10. BISCHOF, J. C.; HE, X., Thermal stability of proteins. *Annals of the New York Academy of Sciences* **2006,** *1066* (1), 12-33.

11. Daniel, R. M., The upper limits of enzyme thermal stability. *Enzyme and Microbial Technology* **1996,** *19* (1), 74-79.

12. Haki, G. D.; Rakshit, S. K., Developments in industrially important thermostable enzymes: a review. *Bioresour Technol* **2003,** *89* (1), 17-34.

13. Prakash, O.; Jaiswal, N., alpha-Amylase: an ideal representative of thermostable enzymes. *Appl Biochem Biotechnol* **2010,** *160* (8), 2401-14.

14. Arnold, F. H., Directed Evolution: Bringing New Chemistry to Life. *Angew Chem Int Ed Engl* **2018,** *57* (16), 4143-4148.

15. Badenhorst, C. P. S.; Bornscheuer, U. T., Getting Momentum: From Biocatalysis to Advanced Synthetic Biology. *Trends Biochem Sci* **2018,** *43* (3), 180-198.

16. Rothlisberger, D.; Khersonsky, O.; Wollacott, A. M.; Jiang, L.; DeChancie, J.; Betker, J.; Gallaher, J. L.; Althoff, E. A.; Zanghellini, A.; Dym, O.; Albeck, S.; Houk, K. N.; Tawfik, D. S.; Baker, D., Kemp elimination catalysts by computational enzyme design. *Nature* **2008,** *453* (7192), 190-5.

17. Kent, S. B., Total chemical synthesis of proteins. *Chem Soc Rev* **2009,** *38* (2), 338-51.

18. Murakami, Y.; Kikuchi Ji, J. I.; Hisaeda, Y.; Hayashida, O., Artificial Enzymes. *Chem. Rev.* **1996,** *96* (2), 721-758.

19. Harris, J. M.; Chess, R. B., Effect of pegylation on pharmaceuticals. *Nat. Rev. Drug Discov.* **2003,** *2* (3), 214-21.

20. Hwang, E. T.; Gu, M. B., Enzyme stabilization by nano/microsized hybrid materials. *Engineering in Life Sciences* **2013,** *13* (1), 49-61.

21. Gauthier, M. A.; Klok, H.-A., Polymer–protein conjugates: an enzymatic activity perspective. *Polymer Chemistry* **2010,** *1* (9), 1352-1373.

22. Pelegri-O'Day, E. M.; Maynard, H. D., Controlled Radical Polymerization as an Enabling Approach for the Next Generation of Protein-Polymer Conjugates. *Accounts Chem. Res.* **2016,** *49* (9), 1777-85.

23. Ju, Y.; Zhang, Y.; Zhao, H., Fabrication of Polymer-Protein Hybrids. *Macromol Rapid Commun* **2018,** *39* (7), e1700737.

24. Henze, M.; Madge, D.; Prucker, O.; Ruhe, J., "Grafting Through": Mechanistic Aspects of Radical Polymerization Reactions with Surface-Attached Monomers. *Macromolecules* **2014,** *47* (9), 2929-2937.

25. Lele, B. S.; Murata, H.; Matyjaszewski, K.; Russell, A. J., Synthesis of uniform protein-polymer conjugates. *Biomacromolecules* **2005,** *6* (6), 3380-7.

26. Tao, L.; Mantovani, G.; Lecolley, F.; Haddleton, D. M., Alpha-aldehyde terminally functional methacrylic polymers from living radical polymerization: application in protein conjugation "pegylation". *J Am Chem Soc* **2004,** *126* (41), 13220-1.

27. Nicolas, J.; San Miguel, V.; Mantovani, G.; Haddleton, D. M., Fluorescently tagged polymer bioconjugates from protein derived macroinitiators. *Chem Commun (Camb)* **2006,** (45), 4697-9.

28. Li, H. M.; Li, M.; Yu, X.; Bapat, A. P.; Sumerlin, B. S., Block copolymer conjugates prepared by sequentially grafting from proteins via RAFT. *Polymer Chemistry* **2011,** *2* (7), 1531-1535.

29. Helal, R.; Melzig, M. F., Determination of lysozyme activity by a fluorescence technique in comparison with the classical turbidity assay. *Pharmazie* **2008,** *63* (6), 415-9.

30. Greenwald, R. B.; Yang, K.; Zhao, H.; Conover, C. D.; Lee, S.; Filpula, D., Controlled release of proteins from their poly(ethylene glycol) conjugates: drug delivery systems employing 1,6-elimination. *Bioconjug Chem* **2003,** *14* (2), 395-403.

31. Yadavalli, N. S.; Borodinov, N.; Choudhury, C. K.; Quiñones-Ruiz, T.; Laradji, A. M.; Tu, S.; Lednev, I. K.; Kuksenok, O.; Luzinov, I.; Minko, S., Thermal Stabilization of Enzymes with Molecular Brushes. *ACS Catalysis* **2017,** *7* (12), 8675-8684.

32. Ji, X. T.; Liu, L.; Zhao, H. Y., The synthesis and self-assembly of bioconjugates composed of thermally-responsive polymer chains and pendant lysozyme molecules. *Polymer Chemistry* **2017,** *8* (18), 2815-2823.

33. Heredia, K. L.; Bontempo, D.; Ly, T.; Byers, J. T.; Halstenberg, S.; Maynard, H. D., In situ preparation of protein-"smart" polymer conjugates with retention of bioactivity. *J Am Chem Soc* **2005,** *127* (48), 16955-60.

34. Choudhury, C. K.; Tu, S.; Luzinov, I.; Minko, S.; Kuksenok, O., Designing Highly Thermostable Lysozyme-Copolymer Conjugates: Focus on Effect of Polymer Concentration. *Biomacromolecules* **2018,** *19* (4), 1175-1188.

35. Haupt, B.; Neumann, T.; Wittemann, A.; Ballauff, M., Activity of enzymes immobilized in colloidal spherical polyelectrolyte brushes. *Biomacromolecules* **2005,** *6* (2), 948-55.

36. Kudina, O.; Zakharchenko, A.; Trotsenko, O.; Tokarev, A.; Ionov, L.; Stoychev, G.; Puretskiy, N.; Pryor, S. W.; Voronov, A.; Minko, S., Highly efficient phase boundary biocatalysis with enzymogel nanoparticles. *Angew Chem Int Ed Engl* **2014,** *53* (2), 483-7.

37. Zakharchenko, A.; Guz, N.; Laradji, A. M.; Katz, E.; Minko, S., Magnetic field remotely controlled selective biocatalysis. *Nat Catal* **2018,** *1* (1), 73-81.

38. Ehlers, J.-E.; Rondan, N. G.; Huynh, L. K.; Pham, H.; Marks, M.; Truong, T. N., Theoretical study on mechanisms of the epoxy− amine curing reaction. *Macromolecules* **2007,** *40* (12), 4370-4377.

39. Kuznetsova, I. M.; Turoverov, K. K.; Uversky, V. N., What macromolecular crowding can do to a protein. *Int J Mol Sci* **2014,** *15* (12), 23090-140.

40. Ellis, R. J., Macromolecular crowding: an important but neglected aspect of the intracellular environment. *Curr Opin Struct Biol* **2001,** *11* (1), 114-9.

41. Feig, M.; Yu, I.; Wang, P. H.; Nawrocki, G.; Sugita, Y., Crowding in Cellular Environments at an Atomistic Level from Computer Simulations. *J Phys Chem B* **2017,** *121* (34), 8009-8025.

42. Gorensek-Benitez, A. H.; Smith, A. E.; Stadmiller, S. S.; Perez Goncalves, G. M.; Pielak, G. J., Cosolutes, Crowding, and Protein Folding Kinetics. *J Phys Chem B* **2017,** *121* (27), 6527-6537.

43. Politou, A.; Temussi, P. A., Revisiting a dogma: the effect of volume exclusion in molecular crowding. *Curr Opin Struct Biol* **2015,** *30*, 1-6.

44. Hong, J.; Gierasch, L. M., Macromolecular crowding remodels the energy landscape of a protein by favoring a more compact unfolded state. *J Am Chem Soc* **2010,** *132* (30), 10445-52.

45. Zhou, H. X., Polymer crowders and protein crowders act similarly on protein folding stability. *FEBS Lett* **2013,** *587* (5), 394-7.

46. Wang, Y.; Sarkar, M.; Smith, A. E.; Krois, A. S.; Pielak, G. J., Macromolecular crowding and protein stability. *J Am Chem Soc* **2012,** *134* (40), 16614-8.

47. Senske, M.; Tork, L.; Born, B.; Havenith, M.; Herrmann, C.; Ebbinghaus, S., Protein stabilization by macromolecular crowding through enthalpy rather than entropy. *J Am Chem Soc* **2014,** *136* (25), 9036-41.

48. Benton, L. A.; Smith, A. E.; Young, G. B.; Pielak, G. J., Unexpected effects of macromolecular crowding on protein stability. *Biochemistry* **2012,** *51* (49), 9773-5.

49. Rodriguez-Martinez, J. A.; Rivera-Rivera, I.; Griebenow, K., Prevention of benzyl alcohol-induced aggregation of chymotrypsinogen by PEGylation. *J Pharm Pharmacol* **2011,** *63* (6), 800-5.

50. Plesner, B.; Fee, C. J.; Westh, P.; Nielsen, A. D., Effects of PEG size on structure, function and stability of PEGylated BSA. *Eur J Pharm Biopharm* **2011,** *79* (2), 399-405.

51. Lawrence, P. B.; Price, J. L., How PEGylation influences protein conformational stability. *Curr Opin Chem Biol* **2016,** *34*, 88-94.

52. Lucius, M.; Falatach, R.; McGlone, C.; Makaroff, K.; Danielson, A.; Williams, C.; Nix, J. C.; Konkolewicz, D.; Page, R. C.; Berberich, J. A., Investigating the Impact of Polymer Functional Groups on the Stability and Activity of Lysozyme-Polymer Conjugates. *Biomacromolecules* **2016,** *17* (3), 1123-34.

53. Lee, L. L.; Lee, J. C., Thermal stability of proteins in the presence of poly(ethylene glycols). *Biochemistry* **1987,** *26* (24), 7813-9.

54. Crowley, P. B.; Brett, K.; Muldoon, J., NMR spectroscopy reveals cytochrome c-poly(ethylene glycol) interactions. *Chembiochem* **2008,** *9* (5), 685-8.

55. Paturej, J.; Sheiko, S. S.; Panyukov, S.; Rubinstein, M., Molecular structure of bottlebrush polymers in melts. *Sci Adv* **2016,** *2* (11), e1601478.

56. Feuz, L.; Leermakers, F. A. M.; Textor, M.; Borisov, O., Bending rigidity and induced persistence length of molecular bottle brushes: A self-consistent-field theory. *Macromolecules* **2005,** *38* (21), 8891-8901.

# CHAPTER 3

# MECHANISM OF POLYETHYLENE GLYCOL CROWDING EFFECT ON LYSOZYME THERMAL STABILITY[1]

[1] Wang, X.; Bowman, J.; Tu, S.; Nykypanchuk, D.; Kuksenok, O.; Minko, S. To be submitted to Biomacromolecules

**Abstract**

We report a mechanism study of the polyethylene glycol (PEG) crowding effect on the thermal stability of hen egg white lysozyme (LYZ). LYZ was mixed with PEG in different concentrations (10 to 100 mg/ml) and molecular weights (Mw=3,350 and 10,000 g/mol) to illustrate the influence on thermal stability. The results demonstrated that with the PEG addition, LYZ residual activity was improved from 15% to 55% after 1 hour incubation at 80°C. The improvement resulted from the reduction in lysozyme aggregations at the elevated temperature according to the formation of PEG-LYZ associates.

**Keywords**: Polyethylene glycol, crowding effect, enzyme catalysis, thermal stability

## Introduction

Industrial and biomedical applications of enzymes continue to expand because of their catalytic efficiency and selectivity[1-6]. Many mesophilic enzymes have poor thermal stability, which leads to limitations for the applications when extended performance at elevated temperatures is beneficial to increase productivity and decrease bacterial contamination of the industrial processes.[7] Most enzymes denature at temperatures above 50-60°C[8-10]. Even, at room temperature, some enzyme undergoes denaturing which affect their shelf life that limits their applications. Simple and cost-efficient methods to improve enzyme stability is highly demanded.

Hen egg white lysozyme (LYZ) is a monomeric protein consisting of 129 amino acid residues and crosslinked by four disulfide bridges[11]. The mechanism of LYZ thermal denaturation can be depicted by the classical scheme of Lumry and Eyring[12]: $N \rightleftarrows U \rightarrow I$, where the native enzyme, N, reversibly unfolded to denatured state, U, following by irreversible transition to an inactive conformation, I. The denaturing process is pH dependent. LYZ can be

irreversibly inactivated at 100°C as a result of deamidation of asparagine residues at pH 4[13, 14], and a combination of aggregation and intermolecular/intramolecular disulfide exchanges (disulfide scrambling) at neutral pH (a range of pH from pH 6 to pH 8)[15]. The maximum LYZ thermal stability was measured at pH 5. The secondary structure of lysozyme is dominated by α-helixes and minor β-sheets and turns. With a progressive rise of temperature, the α-helix structure unfolds. These conformational changes are followed by aggregation of the enzyme and irreversible loss of activity.

It was found that at pH 5, LYZ demonstrated minimal changes in the secondary structure with a minimal aggregation, hence with maximal stability in a temperature range from room temperature to 70°C[16]. The aggregation via the interaction between hydrophobic fragments of the unfolded enzyme remains irreversible upon cooling or dilution[17, 18]. LYZ molecules begin to unfold at around 50°C and then aggregate at about 70°C. At the latter stage, protein globules are denatured and aggregated[19]. Disulfide scrambling, which takes place at neutral to alkaline pH[15, 20], is also accompanied by aggregation[21].

The major energy contribution that stabilizes protein globule dissolved in an aqueous solution comes from the hydrophobic effect[22]. With temperature increase, the hydrophobic effect is weakened, and water molecules penetrate the globule, causing degradation of the secondary structure. Numerous approaches have been proposed to address the problem of proteins' thermal stability. All the methods could be broken down into two large groups. The first group is the development of synthetic proteins through a modification of the genetic code [23-25]. The second group is based on the binding of protein molecules with organic molecules (mainly with polymers)[26] or solid particles (often porous structures)[27]. Both methods are essential because neither of the methods can be universally applied for different applications of proteins. In this

paper, we are interested in the second method, specifically in the mechanism of improvement of the protein stability via interactions with polymeric additives. Protein-polymers systems are interesting for two aspects: (i) improvement of protein stability for storage, transportation, and biotechnological processes at elevated temperatures; (ii) for the understanding of protein interactions in a complex natural or synthetic environment that include natural or synthetic biomacromolecules when, for example, proteins are used as drugs or grows factors for cell culturing

Our previous studies of LYZ-polymer hybrids have illustrated significant improvement of enzyme thermal stability at pH 5.2 [28,29]. In this work, LYZ was conjugated with polyethylene oxide (PEO) bottle-brush through covalently bonded to the backbone of the bottle brush in-between side PEO chains. The half-life of lysozyme polymer conjugate (LPC) at 90°C was extended 9-fold. The possible explanation of the improved enzyme performance is the so called "crowding effect" caused by PEG side chains.

The crowding effect is broadly discussed in the literature for different systems; the PEG-LYZ system is one that among mostly studied. The crowding effect received its name because it is observed at higher concentrations of the crowder – molecules present in solution along with the enzyme. In general, many results are contradictive, showing both improvement [30, 31] or no to negative effects on the thermal stability[32, 33]. For example, the addition of dextran-70 was reported to increase the Tm (the midpoint temperature of denaturation curve) of LYZ[34, 35], but the presence of polyethylene glycol (PEG) resulted in a decrease of the enzyme unfolding temperature[36]. The addition of a block copolymer of PEO and propylene oxide (PPO) resulted in an increase in the refolding yield of denatured LYZ. The increased stability in the latter case was

explained by hydrophobic interactions between LYZ and PPO blocks, while only PEO didn't show any improvement of thermal stability[37].

Generally, crowding effects arise from two-body repulsion at high concentrations of the crowder that stabilize the compact globular conformation of proteins. [38-40] Intermolecular interactions can either amplify or offset the crowding effect. For example, it was proposed that stronger interactions of the crowder with the unfolded protein could offset the two-body repulsion effect[41]. However, this general consideration should be adapted to the specific protein-crowder system. On one side, protein and most crowder molecules are amphiphilic molecules affecting the level of intermolecular interactions through hydrogen bonds, Coulomb interactions, and hydrophobic effect. On the other side, proteins undergo different denaturing mechanisms. Specifically, LYZ undergoes conformation changes at elevated temperatures, which results in irreversible aggregation due to a combination of hydrophobic interactions and disulfide scrambling. In this case, two-body repulsion could result in the irreversible loss of the enzyme activity.

Temperature and concentration of the crowders are important characteristics for the crowding effect. If the crowder is a flexible polymer, the two-body repulsion will increase starting at the coil overlap concentration – at the transition point between diluted and semidiluted polymer solution. Coils size will decrease then until the concentrated solution regime. The temperature dependent interactions of the polymer with the solvent and enzyme will affect the balance of intermolecular interactions and, consequently, the phase behavior in the system.

In this work, we combine experiment and molecular simulation to explain the mechanism behind the crowding effect for LYZ-PEG aqueous solutions. Although this work is specific for the protein and crowder, it will provide a representative example of a combination of different

effects on the thermal stability of proteins. We monitor thermal stability using different approaches, including conformational changes of LYZ, PEG, aggregation, and catalytic activity of the enzyme to obtain a full picture of the changes.

**Experimental Section**

**Materials**. Lysozyme from chicken egg white (LYZ), polyethylene glycol (PEG) Mw=3,350 g/mol (PEG3k), and PEG Mw=10,000g/mol (PEG10k) were purchased from Sigma-Aldrich. An EnzChek fluorescence-based lysozyme assay kit (Catalog No. E22013) was purchased from Thermo Fischer Scientific.

**Enzyme solutions.** 200μg/ml LYZ solutions with 0 to 100mg/ml of PEG3k and 0 to 50mg/ml of PEG10k were prepared in phosphate-buffered saline (PBS) pH=7.4. Lysozyme polymer conjugation solutions were prepared as reported with LYZ concentration at 200μg/ml [28].

**Enzyme activity, thermal stability, and biocatalytic kinetics**. 60μl of LYZ and LYZ+PEG solutions were incubated at room temperature or 80°C for 1 hour. The solutions were then diluted 25 times with PBS. Activity and biocatalytic kinetics were measured with EnzCheck lysozyme assay kit in PBS as previously reported[29].

**Circular Dichroism (CD) Spectroscopy.** CD measurements were carried out with a Jasco J-710 spectra polarimeter for LYZ, LYZ+PEG samples using a quartz cuvette with a path length of 0.1cm. Enzyme concentrations were 15μM for all samples. The spectra were collected in the far-UV regions from 260nm to 190 nm at 1nm bandwidth. The first point was collected at room temperature, then heated up to 80°C and measured every 10 minutes up to 1 hour. The cell was then cooled down to 45°C, and measurements were taken every 10 minutes up to 1 hour. Three scans were averaged for each spectrum. Buffer impact was subtracted properly.

**Lysozyme aggregation percentage.** LYZ and LYZ+PEG solutions were heated at 80°C for 1hour separately, followed by filtration with 50kDa cut-off Amicon® ultra-4 centrifugal filters (Millipore UFC805024) after cooling to room temperature. The enzyme concentrations of filtrates were measured by UV-Vis at 280nm with extinction coefficient 38,940$cm^{-1}M^{-1}$and compared with original solutions at room temperature.

**LYZ size measurement.** Enzymes and polymer sizes were measured with dynamic light scattering (DLS) Zetasize Nano-ZS. LYZ and LYZ+PEG sizes were first collected at 25°C, then heated up to 80°C and collected again. Three measurements were averaged for each data point.

**Small Angle X-ray Scattering (SAXS).** SAXS measurements were performed on a custom built instrument (Saxslab, MA) equipped with a copper rotating anode and 300K Pilatus area detector. We used 0.6 m nominal sample to detector distance; the actual distance was calibrated with Silver Behenate. Data reduction was performed with guisaxs (guisaxs.com) software. Temperature control was performed with an adapted Linkam HFSX350 stage.

For the measurement, the samples were placed in 1mm diameter capillaries (Charles Supper Company, MA) and sealed. The exposure time for temperature controlled measurements was kept at 1 hr (unless otherwise indicated) and we used 0.1 degrees per second for temperature ramp. The equilibration time at each temperature was set to two minutes; longer equilibration times were not necessary due to long exposure times. Data fitting are done using Irena SAXS fitting package[42].

## Results

**Thermal stability in terms of catalytic activity.** Effect of PEG on LYZ stability was conducted with two PEG crowders, PEG3k (critical overlap concentration of 122 mg/ml) and

PEG10k (critical overlap concentration of 54.4mg/ml) at 0-140 mg/ml and 0-60 mg/ml, respectively. After incubation at 80°C for 1 hour, native LYZ (control) was dramatically denatured with only 15% residual activity. The addition of 20mg/ml of PEG3k has enhanced the residual activity to 25%. The higher concentration of PEG3k has induced higher thermal stability of LYZ, and the improvement achieved saturation at 80mg/ml of PEG3k, where about 40% of residual activity was demonstrated, and no further improvement with PEG3k concentration was observed (Figure 3.1a). The introduction of PEG10k has demonstrated a similar stabilizing tendency, however, at a high efficiency compared to PEG3k. With only 10 mg/ml of PEG10k, the residual activity was increased to 31%, and the plateau of PEG10k improvement was at 40mg/ml of PEG with 55% of residual activity comparing to 15% of native LYZ (Figure 3.1b). Thermal stability of LYZ conjugated to PEG-NHS (Mw=10,000g/mol) ester was also compared with free PEG10k, and results showed that with conjugation, the thermal stability of LYZ could be further enhanced to 80% of the residual activity with only 10mg/ml of PEG ester (Figure 3.1c).

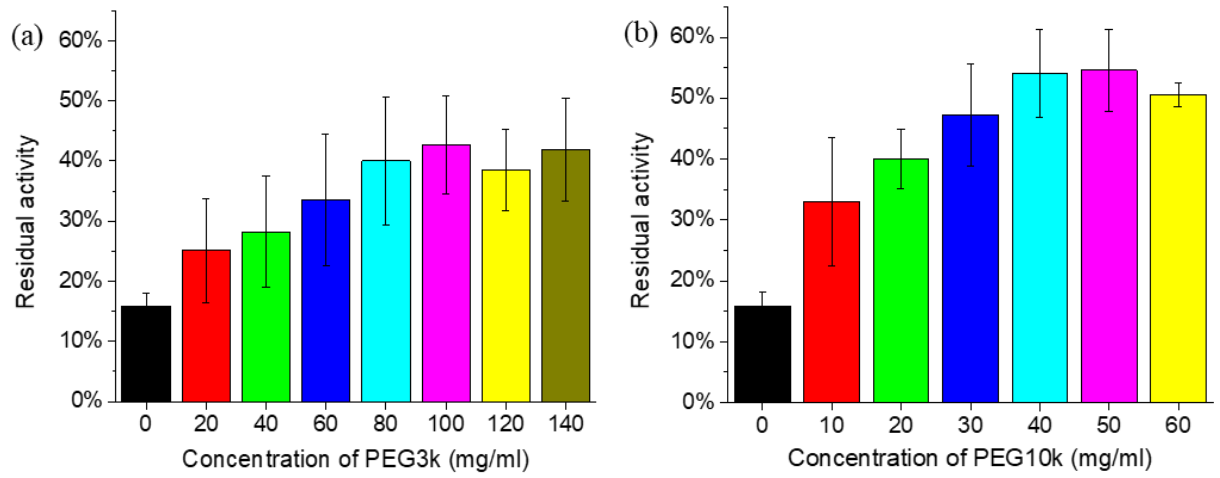

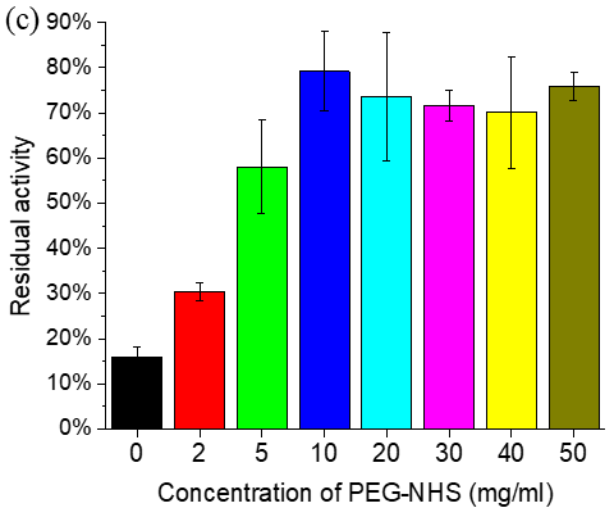


**Figure 3.1** Residual activity of LYZ and LYZ with different concentrations of (a) PEG3k, (b) PEG10k, and (c) PEG-NHS after 1hour incubation at 80°C.

The Michaelis−Menten model was used to analyze biocatalytic kinetics for the native LYZ and LYZ+PEG mixtures (Table 3.1). At room temperature, though both PEG3k and PEG10k showed higher $K_M$ compared to native LYZ, we cannot conclude that PEG has reduced the affinity of LYZ to the substrate, as LYZ+PEGs have shown higher $V_{max}$ as well. A greater turnover number ($k_{cat}$) of LYZ+PEG indicated a higher biocatalytic activity of the LYZ+PEG mixtures at room temperature. After incubation at 80°C, all samples suggested activity reduction owing to enzyme denaturation. But the higher $k_{cat}$ and $k_{cat}/K_M$ in LYZ+PEG mixtures, the better the thermal stabilization compared to LYZ.

**Table 3.1** Kinetic constants for LYZ and LYZ+PEG at RT and after 1-hour Incubation at 80 °C

| | RT | | | | 80°C, 1hr | | | |
|---|---|---|---|---|---|---|---|---|
| | $V_{max}$ (nM/min) | $K_M$ (nM) | $k_{cat}$ ($\times 10^{-4}$ $s^{-1}$) | $k_{cat}/K_M$ ($\times 10^4$ $M^{-1}$ $s^{-1}$) | $V_{max}$ (nM/min) | $K_M$ (nM) | $k_{cat}$ ($\times 10^{-4}$ $s^{-1}$) | $k_{cat}/K_M$ ($\times 10^4$ $M^{-1}$ $s^{-1}$) |
| LYZ | 11.7 ± 0.4 | 28.4 ± 0.3 | 3.5 | 1.2 | 0.6 ± 0.1 | 33.7 ± 0.1 | 0.2 | 0.1 |
| LYZ+ PEG3k | 14.0 ± 0.7 | 31.4 ± 0.5 | 4.2 | 1.3 | 2.0 ± 0.2 | 34.3 ± 0.2 | 0.6 | 0.2 |
| LYZ+ PEG10k | 19.0 ± 0.5 | 44.7 ± 0.5 | 5.7 | 1.3 | 3.9 ± 0.4 | 21.1 ± 0.3 | 1.2 | 0.6 |

**Thermals stability in terms of aggregation.** The denaturation of LYZ is a result of enzyme unfolding and aggregation after high temperature incubation. Dimensions of LYZ and LYZ+PEG were compared at 25°C and 80°C by DLS. The hydrodynamic diameter (HD) of LYZ is 3.1nm as estimated with DLS at room temperature. A rapid aggregation was observed when the LYZ solution was heated up to 80°C, where the HD increased to 212 nm (Table 3.2). HD of LYZ with PEG3k and PEG10k were measured with DLS using the same protocol. As a reference, we used DLS plots obtained for only LYZ and only PEG in solutions. The plots for HD distribution of LYZ and both PEGs overlap in the range of 3-4 nm and cannot be resolved. After incubation at the elevated temperature, both LYZ-PEG mixtures revealed two peaks in DLS plots that correspond to 3.5 nm and 200 nm HD.

The samples of LYZ and LYZ+PEG solutions incubated at the elevated temperature were filtered with 50kDa cut off filters once cooled down to room temperature. The filtrate contained non-aggregated LYZ. Its concentration was estimated with the UV-vis spectrum to calculate

fractions of aggregated LYZ upon incubation at 80°C. The results revealed that 84% of native LYZ, 58% with PEG3k, and 42% with PEG10k was in the form of irreversible aggregates (Table 3.2).

**Table 3.2** LYZ dimensions at 25°C and 80°C and aggregation fraction of LYZ vs. LYZ+PEG after 1-hour incubation at 80°C.

| | HD (nm) | | Aggregation % |
|---|---|---|---|
| | 25°C | 80°C | |
| LYZ | 3.1 ± 0.8 | 211.8 ± 33.0 | 84 ± 6 |
| LYZ+PEG3k | 3.4 ± 0.7 | 3.2 ± 0.4; 163.8 ± 15.3 | 58 ± 9 |
| LYZ+PEG10k | 3.9 ± 0.7 | 4.1 ± 0.4; 208.4 ± 53.8 | 42 ± 11 |
| PEG3k | 2.5 ± 0.6 | 3.3 ± 0.7 | NA |
| PEG10k | 3.8 ± 0.5 | 5.2 ± 0.3 | NA |

**Thermal stability in terms of LYZ conformational changes**. The information about the conformational state of LYZ and LYZ+PEG was collected using circular dichroism (CD) spectra. CD spectrum was first collected at 25°C. Then the samples were heated up to 80°C and measured every 10 min of the 1 hour heating time. The cell was then cooled down to 45°C, and the spectra were collected every 10 min of the 1 hour cooling step. CD spectra for all three samples showed unfolding during heating to 80°C and a fractional recovery of the conformation with cooling down, indicating refolding of LYZ at lower temperatures (Figure 3.2). The secondary structures of LYZ in these samples were analyzed using the BeStSel online computer program[43, 44] for all samples (Figure 3.3). Native LYZ has shown a decrease of concentrations of both helix 1 and 2 at the elevated temperature as the result of LYZ unfolding. The helix 2 structure was partially recovered after cooling, but the helix 1 retained the unfolded

conformation. That implies that the secondary structure is not recovered to the original state and consequently causes the loss of enzyme activity (Figure 3.3a and 3.3b). With the addition of both PEG3k and PEG10k, the helix structures were also partially denatured at 80°C but with much lower margins compared to native LYZ. After cooling down to 45°C, the helix portion recovered to a much higher fraction than LYZ (Figure 3.3a and 3.3b), which is consistent with the LYZ catalytic activity results, where the PEG introduction could stabilize LYZ at elevated temperature. A lower fraction of strands for LYZ+PEG compared to LYZ suggests that the presence of PEG could reduce LYZ aggregation as the presence of β-sheets is a signature of possible aggregations[37] (Figure 3.3c).

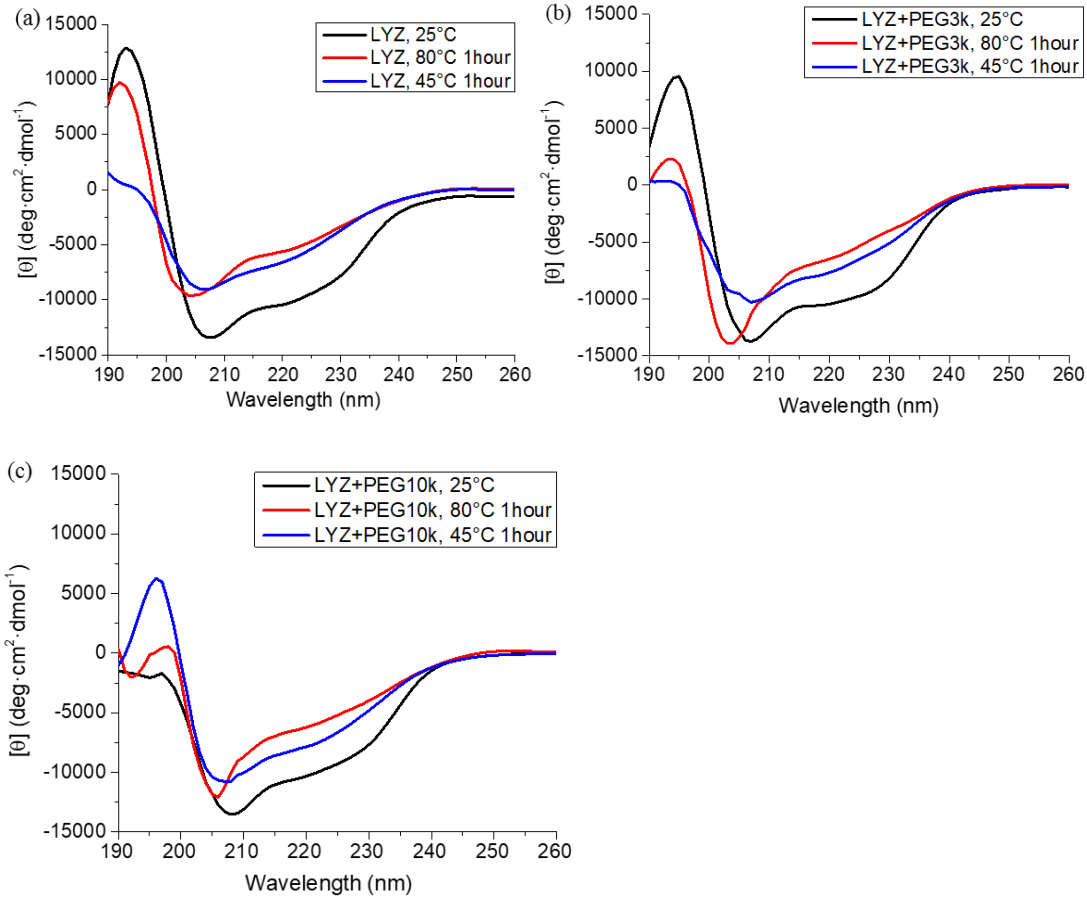


**Figure 3.2** CD spectra of (a)LYZ, (b) LYZ+PEG3k, and (c) LYZ+PEG10k at various temperatures.

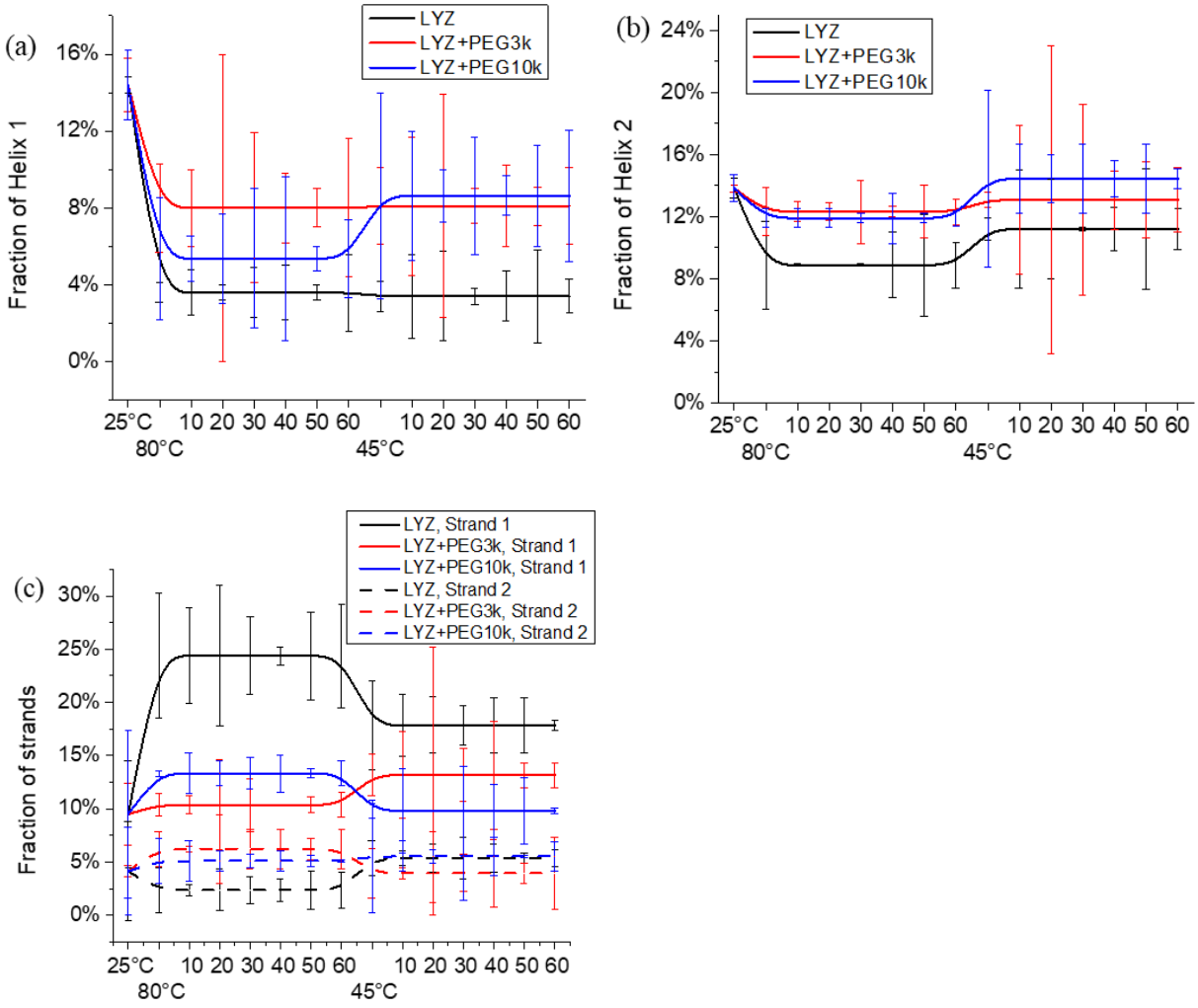


**Figure 3.3** Fraction of secondary structure (a) helix 1, (b) helix 2, and (c) strands for LYZ vs. LYZ+PEG.

**PEG conformational changes and aggregation**. Thermal stability of LYZ and LYZ+PEG mixtures was probed with Small Angle X-ray Scattering (SAXS). Scattering for native lysozyme was satisfactory fitted with a spherical particle model, R = 1.8nm, with a narrow size distribution approaching zero (Table 3.3). Upon heating, the scattering showed both increase in particle size, which could be attributed to partial unfolding, and increase in particle polydispersity to ~27% (gaussian distribution) at 80°C, which decreased to 12% when sample was brought back to room temperature. Upturn in scattering intensity at scattering vectors below

0.03 $A^{-1}$ was indicative of aggregation (Figure 3.4); however, at the measured scattering vector range, we could not obtain the quantitative measurement of aggregate sizes or structure. Based on the scattering intensity change with the temperature and assuming constant scattering contrast of lysozyme, only ~22% of the enzyme remained in the solution.

**Table 3.3** SAXS data fit results for LYZ in PBS

| **Sample** | **$R_g$, nm** | **%** |
|---|---|---|
| Native at 25°C | 1.8 | 100 |
| Heated at 80°C | 2.1 | 35 |
| After heating, cooled to 25°C | 2.1 | 22 |

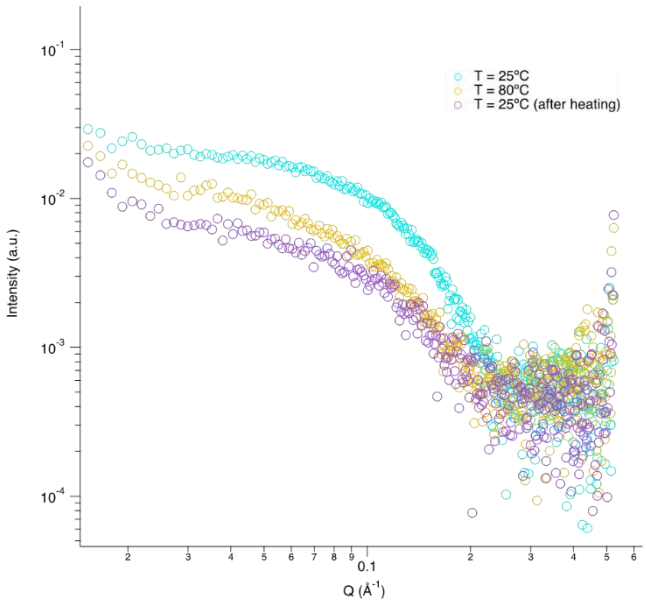


**Figure 3.4** SAXS scattering data for 3mg/ml LYZ solution at 25°C and 80°C.

Similar to LYZ in PBS, scattering data for native LYZ in PEG3k and PEG10k solutions were well described by monodisperse 1.8 nm spherical particles (Table 3.4, Table 3.5). Upon heating, PEG stabilized LYZ in the solution with 66-71% of enzyme retained in the solution in contrast to only 22% without PEG (Table 3.3). For heated samples, the scattering profile could no longer be described by simply increasing polydispersity of particles with Gaussian

distribution, but either required introduction of second population of larger particles (~3nm) in the model, or change to asymmetrical distribution function, such as Lognormal. Using spheroidal model particles improved fit compared to the spherical particles with Gaussian size distribution, but still required introduction of asymmetric size distribution and, in this case, delivered results similar to spheres (Figure 3.5).

Cooling LYZ to room temperature after heating to 80°C showed a reduction of polydispersity for LYZ in the presence of PEG3k, close to the initial state before heating but at the loss of about 30% of the LYZ based on the scattering intensity (Table 3.4).

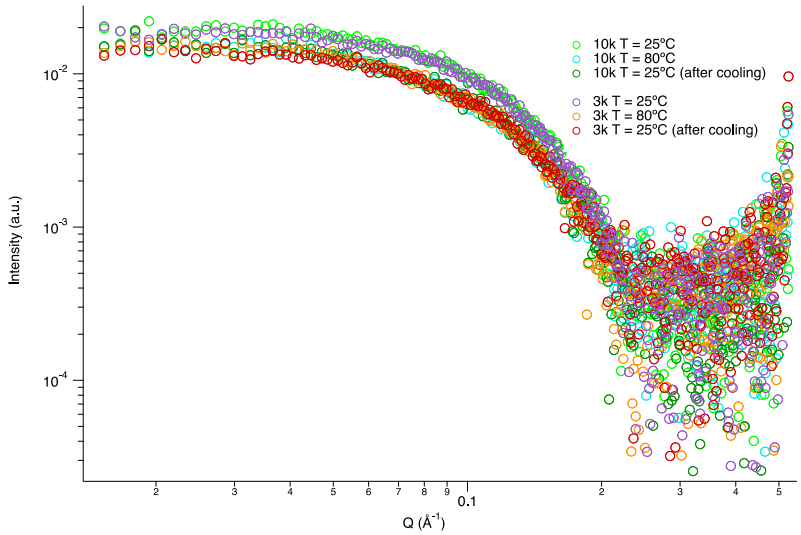


**Figure 3.5** SAXS data for 3mg/ml LYZ solution in 3mg/ml PEG3k and PEG10k solutions at 25°C and 80°C.

**Table 3.4** SAXS data fit results for LYZ in 3mg/ml PEG3k

| **Sample** | **$R_g$, nm** | **%** |
|---|---|---|
| Native at 25°C | 1.8 | 100 |
| Heated at 80°C | 1.7 and 2.9 | 66 |
| After heating, cooled to 25°C | 1.8 | 71 |

**Table 3.5** SAXS data fit results for LYZ in 3mg/ml PEG10k

| **Sample** | **$R_g$, nm** | **%** |
|---|---|---|
| Native at 25°C | 1.8 | 100 |
| Heated at 80°C | 1.8 and 3.2 | 67 |
| After heating, cooled to 25°C | 2.0 | 67 |

25mg/ml PEG10k stabilized LYZ even after 3 hrs of incubation time at 80°C. After cooling from 80 to 25°C, the scattering profile was almost identical to the native LYZ at room temperature (Figure 3.6). However, morphology changes of LYZ were observed at 80°C likely due to partial unfolding. Preliminary fits suggested that scattering was better described by a spheroidal particle with an aspect ratio of 3 rather than a sphere. 30mg/ml of PEG3k improved LYZ thermal stability compared to PBS solution (Figure 3.7). After the heating and cooling cycle, about 41% of the remaining enzyme (estimated from the relative intensity at low Q) in contrast to 22% in PBS solution. Surprisingly the LYZ stability in 30mg/ml PEG3k was lower than that in 3mg/ml PEG3k – which was possibly attributed to the 3 hrs vs. 1 hr incubation time for 30mg/ml and 3mg/ml solutions, respectively.

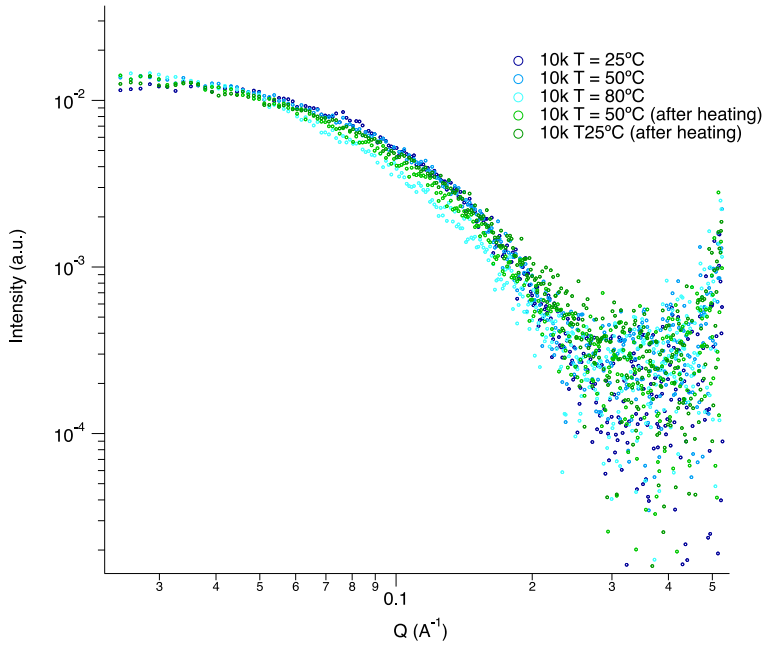


**Figure 3.6** SAXS data for 1.5mg/ml LYZ solution in 25mg/ml PEG10k solution at 25°C, 50°C, and 80°C. Samples were kept for 3hrs at each temperature point.

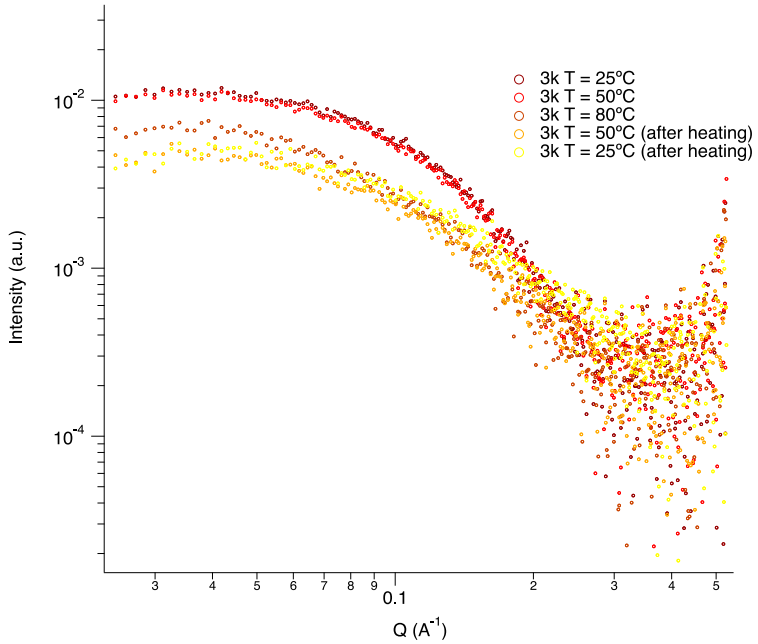


**Figure 3.7** SAXS data for 1.5mg/ml LYZ solution in 30mg/ml PEG3k solution at 25°C, 50°C, and 80°C. Samples were kept for 3hrs at each temperature point.

With small angle x-ray scattering, we could also probe aggregation and change of PEG conformations with temperature (Figure 3.8). At 80°C, scattering intensity increased at small scattering vectors indicating the presence of larger particles in the solution, which illustrated a slight association between PEG molecules (Table 3.6). And the behavior was fully reversible with the temperature (not shown).

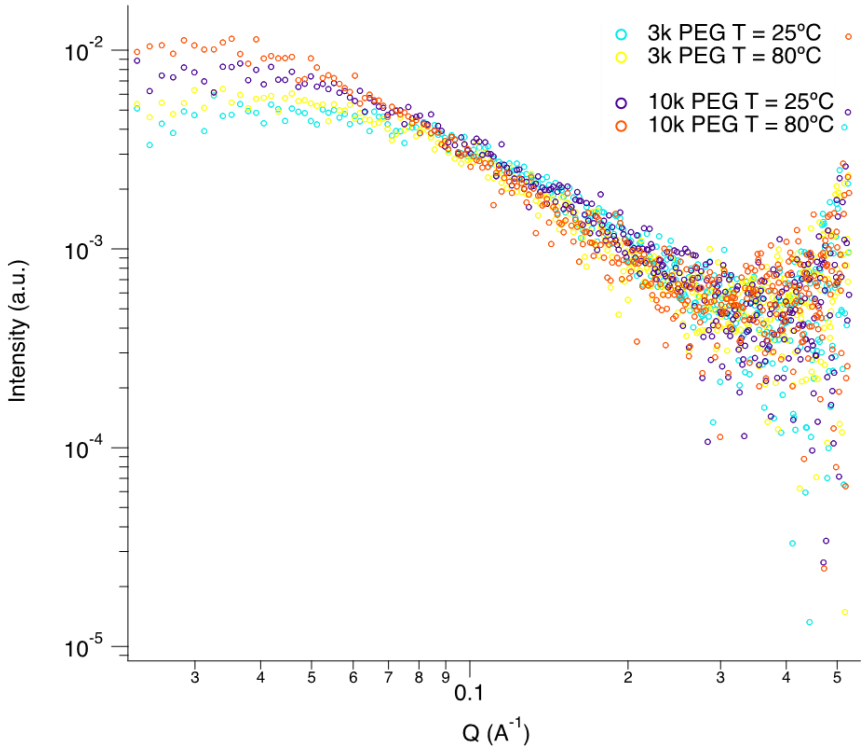


**Figure 3.8** SAXS data of 60mg/ml PEG3k and 50mg/ml PEG10k at 25°C and 80°C.

**Table 3.6** PEG $R_g$ extracted from Gunier-Porod fits

| **Sample** | **$R_g$, nm** |
|---|---|
| PEG3k, 25°C | 1.2 |
| PEG3k, 80°C | 1.5 |
| PEG10k, 25°C | 1.7 |
| PEG10k, 80°C | 2.3 |

SAXS experiments with PEG solutions demonstrated the tendency of PEG aggregation with temperature in a temperature range close to LCST (Figure 3.8). The aggregate dimension

was small yet to cause macroscopic phase separation and precipitation because the experiment was conducted close but below LCST. This tendency was better pronounced for PEG10k than for PEG3k in good agreement with DLS, CD-spectra, and activity tests. Analysis of SAXS data for PEG-LYZ solutions provided the conclusions in good agreement with other methods as well. We observed a strong irreversible aggregation of LYZ at the elevated temperature, while the aggregation was partially reversible for LYZ-PEG10k and LYZ-PEG3k solutions when the stabilizing effect of PEG10k was stronger than PEG3k.

**MD simulation of LYZ-PEG-$H_2O$ concentration and temperature dependent interaction.** MD simulations of LYZ at 500K in an aqueous environment showed an increase in root-mean-square deviation of atoms location (RMSD) (Figure 3.9a) and loss in the number of intra-globular H-bonds (Figure 3.9b), which indicated a strong structural deviation from its initial structure. With the addition of 50% of short PEG chains, a lower RMSD and a higher number of intra H-bonds showed evidence for the stabilizing effect of PEG with the increase of temperature. The greatest stabilizing effect was observed at 90% PEG. The effect of concentration was shifted in simulations to a higher concentration range as compared with that in the experiments because of the computational limitations. The simulations also illustrated that PEG molecules aggregated with the increase of temperature. PEG aqueous solution was characterized by an LCST over 100°C[45]. As temperature rises, the association of PEG molecules increased because it became more hydrophobic. The simulations were conducted for the temperature above LCST. Consequently, we observed phase separation of PEG at 50% concentration, while the system was homogeneous at high PEG concentration, and clear evidence of LYZ-PEG interaction was observed.

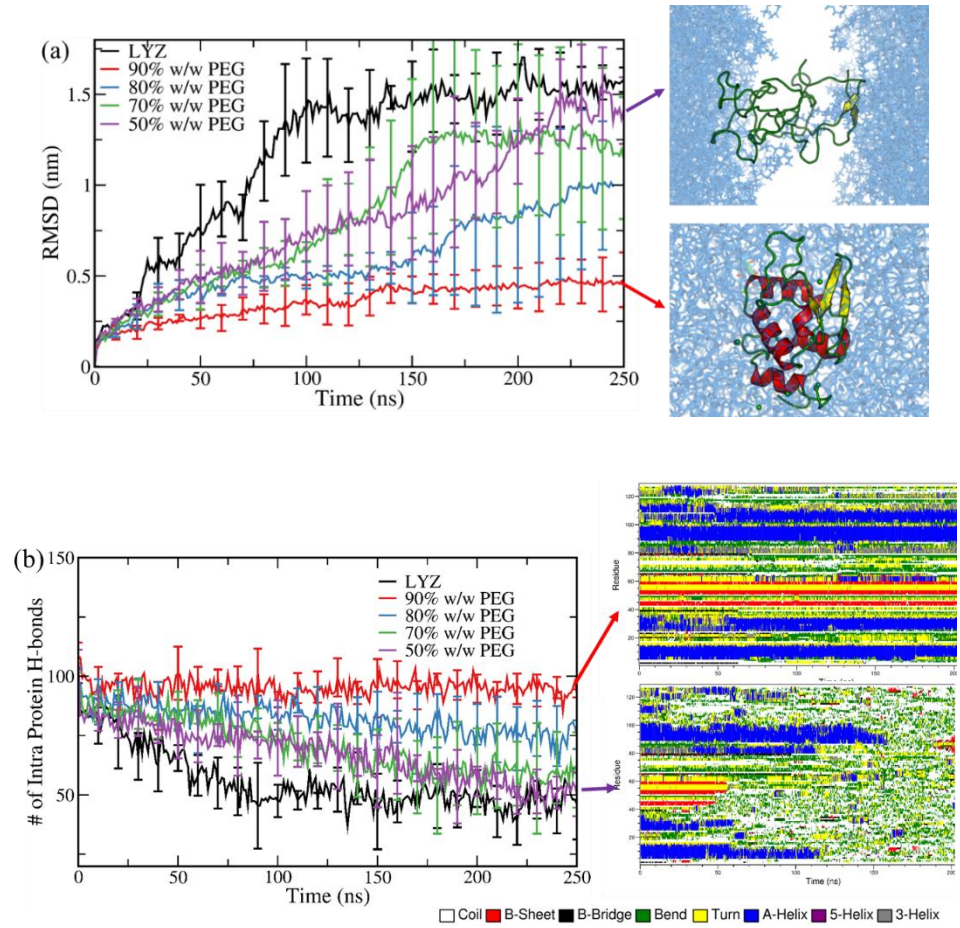


**Figure 3.9** MD simulation results. Time evolution of (a) RMSD and (b) number of intra protein H-bonds at T = 500 K for the native LYZ and LYZ with different amounts of PEG.

## Discussion

Native LYZ denatured at 80°C, pH 7.4 with only 15% of residual activity after 1h incubation, while the addition of PEG had enhanced the activity to up to 55% as concluded from the study of the biocatalytic kinetics (Figure 3.1, Table 3.1). The globules of the native LYZ unfolded at the elevated temperature (Figure 3.2, Figure 3.3) and formed aggregates (Table 3.2, Figure 3.4) due to the hydrophobic effect that resulted in irreversible denaturing and loss of catalytic activity[17].

The improvement of enzyme thermal stability was attributed to stronger hydrophobic interactions of LYZ-PEG, as shown with the MD simulations. The hydrophobic effect resulted in the engulfing of LYZ molecules with PEG, preventing LYZ irreversible aggregation (Table 3.2, Figure 3.6) and water penetration into the globule (Figure 3.9). The impact of this interaction increased with PEG concentration (Figure 3.9) and molecular mass of PEG (Figure 3.7). It saturated at the critical overlap concentration for PEG polymers (Figure 3.1). It is likely that at the critical overlap concentrating, a dense PEG shell was formed around the enzyme.

PEG coils are soft crowder when the two-body repulsion is replaced with a "soft repulsion" affected by the entropy of the PEG coil. However, we observed the domination of the hydrophobic effect over LYZ-PEG coil repulsion.

Once the temperature cooled down, the LYZ-PEG-water interaction restored the initial equilibrium state. The partially unfolded LYZ could refold to the native state and retain the catalytic activity. The conclusion is consistent with the literature reporting that at high temperature, PEG preferentially interacts with the unfolded lysozyme, but is excluded from the native state at low temperature [46].

Covalent conjugation of LYZ with PEG-NHS demonstrated a higher efficiency of the thermal stability due to the stronger interaction between LYZ and PEG. The stability of the conjugated LYZ was increasing with PEG-NHS as well, mainly due to the higher degree of conjugation. This reference experiment underlined the importance of LYZ-PEG interactions for preventing LYZ aggregation.

## Conclusion

PEG crowding effects on LYZ thermal stability had been explored in terms of activity and conformational changes. The PEG addition had enhanced LYZ residual activity from 15% to 55% after 1hour incubation at 80°C. Stabilization effects were related to PEG concentrations and molecular weights. The improvement was attributed to PEG-LYZ interaction at high temperature in suppressing the formation of enzyme aggregations. MD simulations demonstrated strong hydrophobic interactions of LYZ-PEG at the elevated temperature, and CD and SAXS spectra confirmed the formation of LYZ-PEG associates at 80°C.

## References


1. Ansari, S. A.; Husain, Q., Potential applications of enzymes immobilized on/in nano materials: A review. *Biotechnol Adv* **2012,** *30* (3), 512-23.

2. Ariga, K.; Ji, Q.; Mori, T.; Naito, M.; Yamauchi, Y.; Abe, H.; Hill, J. P., Enzyme nanoarchitectonics: organization and device application. *Chem Soc Rev* **2013,** *42* (15), 6322-45.

3. Es, I.; Vieira, J. D.; Amaral, A. C., Principles, techniques, and applications of biocatalyst immobilization for industrial application. *Appl Microbiol Biotechnol* **2015,** *99* (5), 2065-82.

4. Kirk, O.; Borchert, T. V.; Fuglsang, C. C., Industrial enzyme applications. *Current Opinion in Biotechnology* **2002,** *13* (4), 345-351.

5. Min, K.; Yoo, Y. J., Recent progress in nanobiocatalysis for enzyme immobilization and its application. *Biotechnology and Bioprocess Engineering* **2014,** *19* (4), 553-567.

6. Misson, M.; Zhang, H.; Jin, B., Nanobiocatalyst advancements and bioprocessing applications. *J R Soc Interface* **2015,** *12* (102), 20140891.

7. Iyer, P. V.; Ananthanarayan, L., Enzyme stability and stabilization—Aqueous and non-aqueous environment. *Process Biochemistry* **2008,** *43* (10), 1019-1032.

8. Arakawa, T.; Prestrelski, S. J.; Kenney, W. C.; Carpenter, J. F., Factors affecting short-term and long-term stabilities of proteins. *Advanced Drug Delivery Reviews* **1993,** *10* (1), 1-28.

9. BISCHOF, J. C.; HE, X., Thermal stability of proteins. *Annals of the New York Academy of Sciences* **2006,** *1066* (1), 12-33.

10. Daniel, R. M., The upper limits of enzyme thermal stability. *Enzyme and Microbial Technology* **1996,** *19* (1), 74-79.

11. Guez, V.; Roux, P.; Navon, A.; Goldberg, M. E., Role of individual disulfide bonds in hen lysozyme early folding steps. *Protein science* **2002,** *11* (5), 1136-1151.

12. Lumry, R.; Eyring, H., Conformation changes of proteins. *The Journal of physical chemistry* **1954,** *58* (2), 110-120.

13. Ahern, T. J.; Klibanov, A. M., The mechanisms of irreversible enzyme inactivation at 100C. *Science* **1985,** *228* (4705), 1280-1284.

14. Tomizawa, H.; Yamada, H.; Imoto, T., The Mechanism of Irreversible Inactivation of Lysozyme at pH 4 and 100. degree. C. *Biochemistry* **1994,** *33* (44), 13032-13037.

15. Tomizawa, H.; Yamada, H.; Tanigawa, K.; Imoto, T., Effects of Additives on Irreversible Inactivation of Lysozyme at Netral pH and 100° C. *The Journal of Biochemistry* **1995,** *117* (2), 369-373.

16. Venkataramani, S.; Truntzer, J.; Coleman, D. R., Thermal stability of high concentration lysozyme across varying pH: A Fourier Transform Infrared study. *Journal of pharmacy & bioallied sciences* **2013,** *5* (2), 148.

17. Ahern, T. J.; Klibanov, A. M., Analysis of processes causing thermal inactivation of enzymes. *Methods of biochemical analysis* **1988**, 91-128.

18. Raccosta, S.; Manno, M.; Bulone, D.; Giacomazza, D.; Militello, V.; Martorana, V.; San Biagio, P. L., Irreversible gelation of thermally unfolded proteins: structural and mechanical properties of lysozyme aggregates. *European Biophysics Journal* **2010,** *39* (6), 1007-1017.

19. Green, R.; Hopkinson, I.; Jones, R., Unfolding and intermolecular association in globular proteins adsorbed at interfaces. *Langmuir* **1999,** *15* (15), 5102-5110.

20. Steinrauf, L. K.; Dandliker, W. B., A Study of the Reaction of the Disulfide Groups of Bovine Serum Albumin during Heat Denaturation1. *Journal of the American Chemical Society* **1958,** *80* (15), 3833-3835.

21. Yang, M.; Dutta, C.; Tiwari, A., Disulfide-bond scrambling promotes amorphous aggregates in lysozyme and bovine serum albumin. *The Journal of Physical Chemistry B* **2015,** *119* (10), 3969-3981.

22. Schulz, G. E.; Schirmer, R. H., *Principles of protein structure*. Springer Science & Business Media: 2013.

23. Arnold, F. H., Directed Evolution: Bringing New Chemistry to Life. *Angew Chem Int Ed Engl* **2018,** *57* (16), 4143-4148.

24. Badenhorst, C. P. S.; Bornscheuer, U. T., Getting Momentum: From Biocatalysis to Advanced Synthetic Biology. *Trends Biochem Sci* **2018,** *43* (3), 180-198.

25. Rothlisberger, D.; Khersonsky, O.; Wollacott, A. M.; Jiang, L.; DeChancie, J.; Betker, J.; Gallaher, J. L.; Althoff, E. A.; Zanghellini, A.; Dym, O.; Albeck, S.; Houk, K. N.; Tawfik, D. S.; Baker, D., Kemp elimination catalysts by computational enzyme design. *Nature* **2008,** *453* (7192), 190-5.

26. Gauthier, M. A.; Klok, H.-A., Polymer–protein conjugates: an enzymatic activity perspective. *Polymer chemistry* **2010,** *1* (9), 1352-1373.

27. Hwang, E. T.; Gu, M. B., Enzyme stabilization by nano/microsized hybrid materials. *Engineering in Life Sciences* **2013,** *13* (1), 49-61.

28. Yadavalli, N. S.; Borodinov, N.; Choudhury, C. K.; Quiñones-Ruiz, T.; Laradji, A. M.; Tu, S.; Lednev, I. K.; Kuksenok, O.; Luzinov, I.; Minko, S., Thermal Stabilization of Enzymes with Molecular Brushes. *ACS Catalysis* **2017,** *7* (12), 8675-8684.

29. Wang, X.; Yadavalli, N. S.; Laradji, A. M.; Minko, S. J. M., Grafting through Method for Implanting of Lysozyme Enzyme in Molecular Brush for Improved Biocatalytic Activity and Thermal Stability. *Macromolecules* **2018,** *51* (14), 5039-5047.

30. Eggers, D. K.; Valentine, J. S., Molecular confinement influences protein structure and enhances thermal protein stability. *Protein Science* **2001,** *10* (2), 250-261.

31. Kuznetsova, I. M.; Turoverov, K. K.; Uversky, V. N., What macromolecular crowding can do to a protein. *International journal of molecular sciences* **2014,** *15* (12), 23090-23140.

32. Sadhukhan, N.; Muraoka, T.; Ui, M.; Nagatoishi, S.; Tsumoto, K.; Kinbara, K., Protein stabilization by an amphiphilic short monodisperse oligo (ethylene glycol). *Chemical Communications* **2015,** *51* (40), 8457-8460.

33. Zhang, D.-L.; Wu, L.-J.; Chen, J.; Liang, Y., Effects of macromolecular crowding on the structural stability of human α-lactalbumin. *Acta Biochim Biophys Sin* **2012,** *44* (8), 703-711.

34. Sasahara, K.; McPhie, P.; Minton, A. P., Effect of dextran on protein stability and conformation attributed to macromolecular crowding. *Journal of molecular biology* **2003,** *326* (4), 1227-1237.

35. Ghosh, S.; Shahid, S.; Raina, N.; Ahmad, F.; Hassan, M. I.; Islam, A., Molecular and macromolecular crowding-induced stabilization of proteins: Effect of dextran and its building block alone and their mixtures on stability and structure of lysozyme. *International journal of biological macromolecules* **2019**.

36. Zielenkiewicz, W.; Swierzewski, R.; Attanasio, F.; Rialdi, G., Thermochemical, volumetric and spectroscopic properties of lysozyme–poly (ethylene) glycol system. *Journal of thermal analysis and calorimetry* **2006,** *83* (3), 587-595.

37. Chin, J.; Mustafi, D.; Poellmann, M. J.; Lee, R. C., Amphiphilic copolymers reduce aggregation of unfolded lysozyme more effectively than polyethylene glycol. *Physical biology* **2017,** *14* (1), 016003.

38. Ralston, G., Effects of" crowding" in protein solutions. *Journal of chemical education* **1990,** *67* (10), 857.

39. Politou, A.; Temussi, P. A., Revisiting a dogma: the effect of volume exclusion in molecular crowding. *Curr Opin Struct Biol* **2015,** *30*, 1-6.

40. Hong, J.; Gierasch, L. M., Macromolecular Crowding Remodels the Energy Landscape of a Protein by Favoring a More Compact Unfolded State. *Journal of the American Chemical Society* **2010,** *132* (30), 10445-10452.

41. Wang, Y.; Sarkar, M.; Smith, A. E.; Krois, A. S.; Pielak, G. J., Macromolecular crowding and protein stability. *Journal of the American Chemical Society* **2012,** *134* (40), 16614-16618.

42. Ilavsky, J.; Jemian, P. R., Irena: tool suite for modeling and analysis of small-angle scattering. *Journal of Applied Crystallography* **2009,** *42* (2), 347-353.

43. Micsonai, A.; Wien, F.; Kernya, L.; Lee, Y.-H.; Goto, Y.; Réfrégiers, M.; Kardos, J., Accurate secondary structure prediction and fold recognition for circular dichroism spectroscopy. *Proceedings of the National Academy of Sciences* **2015,** *112* (24), E3095-E3103.

44. Micsonai, A.; Wien, F.; Bulyáki, É.; Kun, J.; Moussong, É.; Lee, Y.-H.; Goto, Y.; Réfrégiers, M.; Kardos, J., BeStSel: a web server for accurate protein secondary structure prediction and fold recognition from the circular dichroism spectra. *Nucleic acids research* **2018,** *46* (W1), W315-W322.

45. Saeki, S.; Kuwahara, N.; Nakata, M.; Kaneko, M., Upper and lower critical solution temperatures in poly (ethylene glycol) solutions. *Polymer* **1976,** *17* (8), 685-689.

46. Lee, L. L.; Lee, J. C., Thermal stability of proteins in the presence of poly (ethylene glycols). *Biochemistry* **1987,** *26* (24), 7813-7819.

# CHAPTER 4

# CREATION OF CELLULASES WITH DNA LINKERS

## Introduction

Cellulosomes are multienzyme complexes either attached or secreted from the cell. Cellulosome from anaerobic thermophilic bacterium *Clostridium thermocellum* was first identified in the early 1980s and defined as a "discrete, cellulose-binding, multienzyme complex that mediates the degradation of cellulosic substrates" [1, 2]. Cellulosomes contain one noncatalytic protein scaffoldin locating with multiple cohesins, and catalytic modules with dockerins are assembled to the scaffoldin through cohesin-dockerin interactions. Most scaffoldins also carry one carbohydrate-binding module (CBM) that can anchor the complex to the cellulose surface[3-6]. *C. thermocellum* cellulosome has shown efficient synergism in solubilizing bacterial and *Valonia* cellulose with 75% and 100% crystallinity separately[7], and the activity of cellulosome against crystalline cellulose is 50-fold higher than the corresponding *Tricoderma* free cellulase system[8, 9]. The synergistic interaction can be attributed to the spatial proximity of enzymes grafted and further augmented by the substrate targeting of CBM[10].

The high efficiency of natural cellulosomes in degrading cellulosic biomass has inspired scientists to develop artificial multienzyme complexes to reconstruct the natural structure. The flexibility of building artificial cellulosomes should be more compatible with industrial applications and could help to investigate the mechanisms of the cellulosome synergy effect.

Cellulosomes mediated by DNA were investigated, leveraging the self-assembling property of DNA strands and convenience in producing controllable structures. An endoglucanase Cel5A from *Thermobifida fusca* was modified onto double-stranded DNA with microbial transglutaminase (MTG) cross linking. The enzymatic saccharification of the complex was up to 5-fold higher than free cellulases on microcrystalline cellulose, but had little improvement on the soluble substrate; however, the positions of enzymes on the scaffold were random without identified organization[11]. DNA-binding cellulases were then introduced to establish position-specific cellulosomes. Two types of zinc-finger proteins (ZFP), Zif268 and PE1A, were used for DNA-protein connections, each of which had a high affinity to the unique 9 base pair (bp) sequence. Two DNA modified cellulases were then assembled onto a complementary DNA template with 2 binding sites forming site-specific cellulosome, resulting in a 1.7-fold enhancement in PASC degradation. The flexibility of DNA design enables more binding sites introduced, and the addition of one CBM or cellulase could further increase the sugar production by 12% and 20% compared to the two-component structure[12]. But the low binding affinity of ZFPs toward DNA limited the efficiency in cellulosome assembling, resulting in only 50% cellulosome established[12]. Generation of four-component artificial cellulosomes using HaloTag was reported to obtain 2.8-fold enhancement in glucose production. Further enhancement of 5.1-fold was attained when the four-component cellulosome assembled on rolling circle amplification (RCA) templates, where up to 200 repeats of the four-component binding sites were displayed[13]. The method could efficiently generate cellulosome with DNA scaffolds; however, the process is relatively complex where expertise in creating enzymes with Halotags and modifying DNA linkers with CH ligand (HaloTag Succinimidyl Ester (O4) Ligand) is essential.

Herein, we propose a straightforward and universal method to modify cellulases/CBM with DNA linkers. Cellulases and CBM were first coupled with azido-$PEG_3$-NHS-ester through lysine amino acid residuals to achieve azide-functional groups. Protein-$N_3$ was then reacted with dibenzocyclooctyne (DBCO) functionalized DNA (DNA-DBCO) to tether a single-stranded DNA over strain-promoted alkyne−azide cycloaddition (SPAAC). The success of DNA labeling was confirmed by electrophoresis.

**Experimental Section**

**Materials**. Endo-1,4-β-D-glucanase from *Thermotoga maritima* (EC 3.2.1.4) (TM) and β-Glucosidase from *Agrobacterium sp*. (EC 3.2.1.21) were purchased from Megazyme. Exo-1,4-β-glucanse from *Thermobifida fusca* (EC 3.2.1.91) (6B) and CBM from *Clostridium thermocellum* were purchased from NZYTech. Dibenzocyclooctyl (DBCO) modified DNA linkers, and DNA templates were ordered from Integrated DNA Technologies. Zeba™ spin desalting columns 7k MWCO (89890, 89892), Pierce™ BCA Protein Assay Kit (23225), and 4-20% Invitrogen™ Novex™ TBE Gels (EC6225BOX) were bought from Fisher Scientific. Vivaspin™ ultrafiltration spin columns and Ni Sepharose High Performance resin (17526801) were ordered from GE Healthcare Life Sciences. Materials used for azido-$PEG_3$-NHS ester preparation were commercially purchased from Sigma Aldrich, Alfa, Fisher, VWR and Oakwood Chemical companies and directly used without purification

**Synthesis of azido-$PEG_3$-NHS ester.** The azido-$PEG_3$-NHS was synthesized through general methods with minor modifications[14-16] (Figure 4.1). The oxa-Michael addition of triethylene glycol and t-butyl acrylate in THF using Na chips as base gave tert-butyl 3-(2-(2-(2-hydroxyethoxy) ethoxy) ethoxy) propanoate **1** in 87% yield. The alcohol group in link **1** was

tosylated in TEA/DCM to produce compound **2** in 77% yield, and then quantitatively converted into azido compound **3** by heating with $NaN_3$ in DMF. The tert-butyl ester in compound **3** was removed using TFA/DCM to produce carboxylic acid **4**, which was then treated with EDC•HCl and NHS to form desired link **5** in 60% yield.

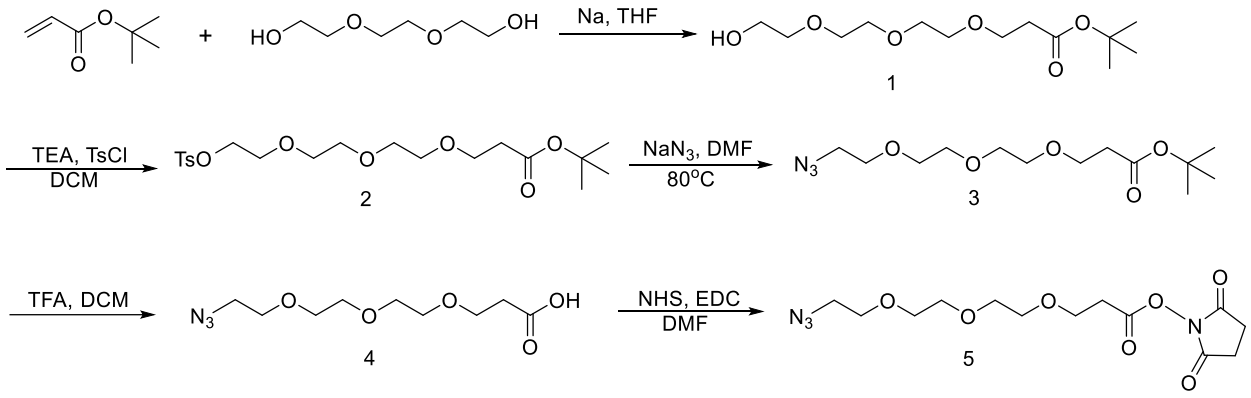


**Figure 4.1** Reaction scheme of Azido-$PEG_3$-NHS synthesis

**Azide modified cellulases/CBM (cellulase/CBM-$N_3$).** 200μg/ml cellulases and CBM solutions were prepared in 100mM sodium phosphate buffer with 100mM NaCl (pH=7). Azido-$PEG_3$-NHS ester was dissolved in dimethyl sulfoxide (DMSO) at 100mg/ml and added into cellulases/CBM solutions at 1000:1 molar ratio to proteins and incubated overnight. The excess ester was removed by Zeba™ spin desalting columns as the manufacturer instructed. Protein concentrations were confirmed with BCA assay.

**Cellulase/CBM conjugated to DNA linkers (cellulase/CBM-DNA).** DNA linkers were dissolved in 100mM sodium phosphate buffer with 100mM NaCl (pH=7) and mixed with cellulase/CBM-$N_3$ solutions at 5:1 molar ratio. The sequences of DNA-DBCO are shown in Table 4.1. The connection of DNA linkers was confirmed by 4-20% TBE gel electrophoresis.

**Table 4.1** List of DNA sequences

| DNA | Sequence |
|---|---|
| Linker 1 | 5'-CCA ACC CAG TCA TGT GTG TTT /3DBCON/-3' |
| Linker 2 | 5'-TAG CAT CCT ACC TGT CCG TTT /3DBCON/-3' |
| Linker 3 | 5'-TAA GCT TGC GAG ACG TCT TTT /3DBCON/-3' |

**Purification of unconjugated DNA-DBCO**. Two methods were processed to remove unconjugated DNA linkers. (1) Spin filtration. Vivaspin™ ultrafiltration spin columns with polyethersulfone (PES) membrane (5k, 10k, and 30k cutoff) were used. The amount of DNA was measured with UV-vis at 260nm, and protein concentrations were obtained by BCA assay. (2) The second method was his-tag purification. All the cellulases and CBM were recombinant enzymes with his-tags, and Ni Sepharose High Performance resin (17526801) was applied as manufacturer instructed in the removal of excess DNA linkers.

**Enzyme activity and CBM binding capability**. Activity assayed with carboxymethyl cellulose (CMC) was processed through incubation of 30µl of 1µM enzyme solution with 30µl of 2% CMC in phosphate buffer at 50°C for 1 hour. The reaction was terminated by immersing the sample tubes in ice water.

Activity against Avicel was measured by incubating 1µM of enzyme solution with 2% Avicel suspension at 50°C for 24hr. The reaction was terminated by immersing in cold water and centrifuge at 10,000×g for 5minutes. Enzyme activity assayed by filter paper was processed as reported [17].

To evaluate reducing sugar concentration, 90µl dinitrosalicylic acid (DNS) solution was added to 60µl of supernatant and boiled for 10 minutes. Optical density was measured at 540 nm, and activity was determined from a glucose standard curve.

## Results and Discussion

The schematic presentation of the synthetic steps for DNA linker conjugation is shown in Figure 4.2. Azide-functional group modified cellulases and CBM were first obtained through coupling between lysine amino acid residuals of the proteins and azido-$PEG_3$-NHS-ester, followed by reaction with dibenzocyclooctyne (DBCO) functionalized DNA to tether a single-stranded DNA to the proteins over strain-promoted alkyne−azide cycloaddition (SPAAC).

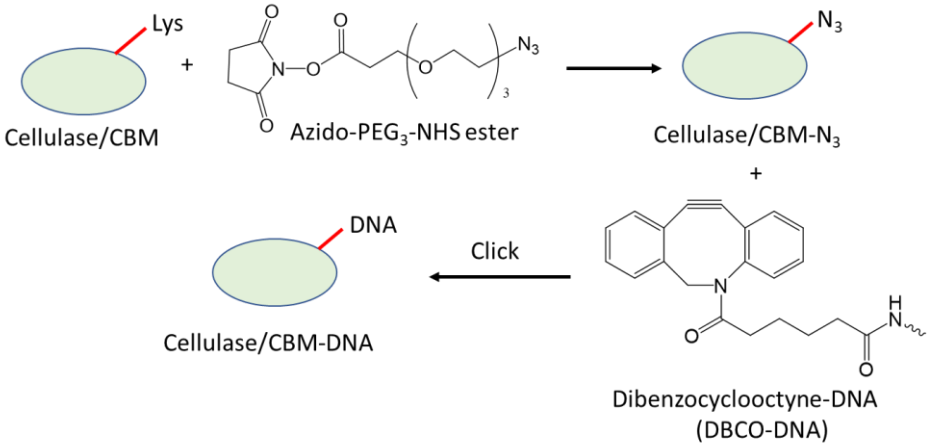


**Figure 4.2** Schematic presentation of synthesis of the cellulosome complex

**Cellulases/CBM conjugated with DNA linkers.** The conjugation of DNA linkers to proteins was confirmed by TBE electrophoresis (Figure 4.3). Free DNA-DBCO and conjugated CBM, TM, and 6B were processed. Comparing to free DNA linkers, all conjugates have shown band shift indicating the successful connection of DNA onto proteins.

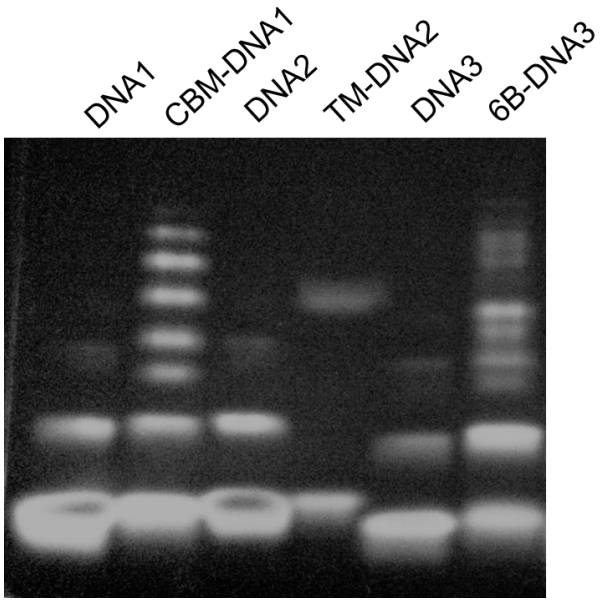


**Figure 4.3** 4-20% TBE electrophoresis for free DNA linkers and cellulase/CBM-DNA conjugates.

**Purification of unconjugated DNA-DBCO.** Spin filtration was initially processed to remove unconjugated DNA-DBCOs. Filters with 5k, 10k, and 30k cutoff were applied at 14000×g for 3-15 minutes with four rounds of washes. DNA concentrations in the filtrate were measured by UV-vis at 260nm (Table 4.2), and only10k and 30k filters could efficiently remove DNA linkers after 4$^{th}$ filtration, but the enzyme concentrations in left-over solutions illustrated low recoveries of proteins (Table 4.3). Centrifugation at 5000×g was processed similarly, demonstrating 10k filter was not efficient in DNA removal, and 30k couldn't avoid protein loss. The results indicated filtration is not a proper method in the purification of excess DNA-DBCOs.

**Table 4.2** Amount of DNA after spin filtration

| | 30k filter | | | | 10k filter | | | | 5k filter | |
|---|---|---|---|---|---|---|---|---|---|---|
| **Speed and time** | **14000×g, 3min** | | **5000×g, 5min** | | **14000×g, 3min** | | **5000×g, 5min** | | **14000×g, 15min** | |
| | **DNA amount (nmol)** | **% DNA** | **DNA amount (nmol)** | **% DNA** | **DNA amount (nmol)** | **% DNA** | **DNA amount (nmol)** | **% DNA** | **DNA amount (nmol)** | **% DNA** |
| **Initial** | 8.79 | Ref | 8.73 | Ref | 8.21 | Ref | 2.81 | Ref | 5.09 | Ref |
| **1st filtrate** | 4.23 | 48% | 1.68 | 19% | 3.00 | 37% | 0.25 | 9% | $7.84\times10^{-2}$ | 2% |
| **2nd filtrate** | 2.28 | 26% | 2.29 | 26% | 2.60 | 32% | 0.28 | 10% | $7.52\times10^{-2}$ | 1% |
| **3rd filtrate** | 1.18 | 13% | 2.41 | 28% | 1.20 | 15% | 0.21 | 7% | $8.85\times10^{-2}$ | 2% |
| **4th filtrate** | 0.60 | 7% | 1.28 | 15% | 0.60 | 7% | 0.18 | 6% | N.A. | N.A. |
| **Retained DNA** | 0.29 | 3% | 0.92 | 11% | 0.81 | 10% | 1.92 | 68% | 4.96 | 97% |

**Table 4.3** Protein concentration after spin filtration

| **Filter size** | **30k filter** | | | | | | **10k filter** | | |
|---|---|---|---|---|---|---|---|---|---|
| **Speed and time** | **14000×g, 3min** | | | **5000×g, 5min** | | | **14000×g, 3min** | | |
| **DNA% in filtrate** | **TM** | **6B** | **CBM** | **TM** | **6B** | **CBM** | **TM** | **6B** | **CBM** |
| **Original protein conc (ug/ml)** | 65.9 | 54.7 | 65.9 | 26.7 | 22.0 | 21.8 | 24.6 | 19.2 | 23.0 |
| **Retained protein conc (ug/ml)** | 10.7 | 7.0 | 6.8 | 0.1 | 14.5 | 4.0 | 1.3 | 17.5 | 2.3 |
| **Retained protein %** | 16% | 13% | 10% | 0.4% | 66% | 19% | 6% | 91% | 10% |

The second purification method was his-tag purifications since all proteins were coded with his-tags. The purified proteins were confirmed by electrophoresis (Figure 4.4). The elimination of lower bands indicated the successful removal of free DNA-DBCO.

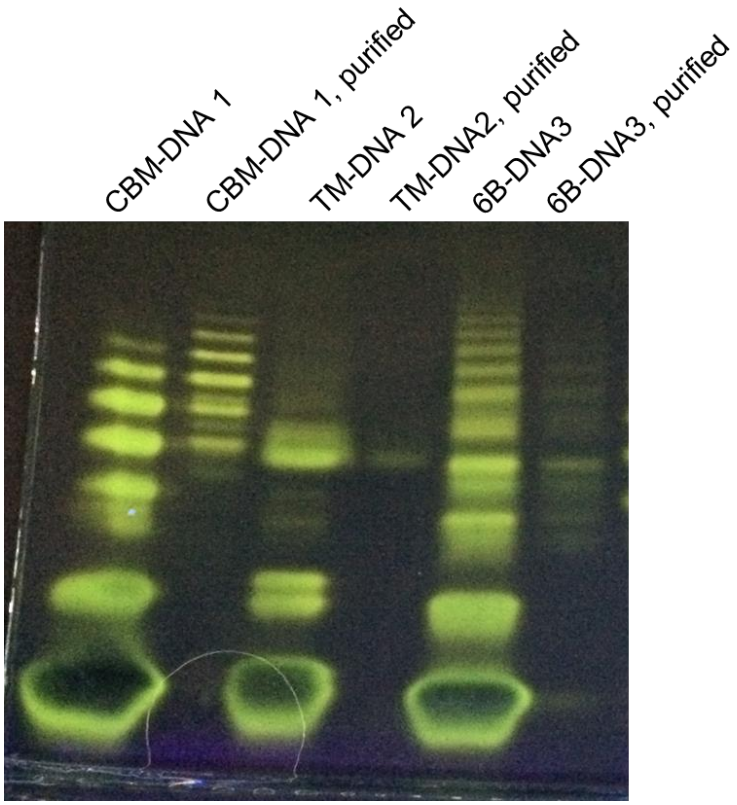


**Figure 4.4** 4-20% TBE electrophoresis for protein-DNA before and after his-tag purification.

**Activity of cellulases and binding capability of CBM after modifications.** Multiple conjugation and purification steps were processed for DNA linker attachment. Since each modification may cause protein property alterations, the activity of cellulases and binding capability of CBM after conjugations were measured to monitor the behavior of enzymes (Figure 4.5). The results demonstrated both TM and 6B could maintain activity similar to initial enzymes; however, the conjugation of DNA has significantly reduced the binding capability of CBM.

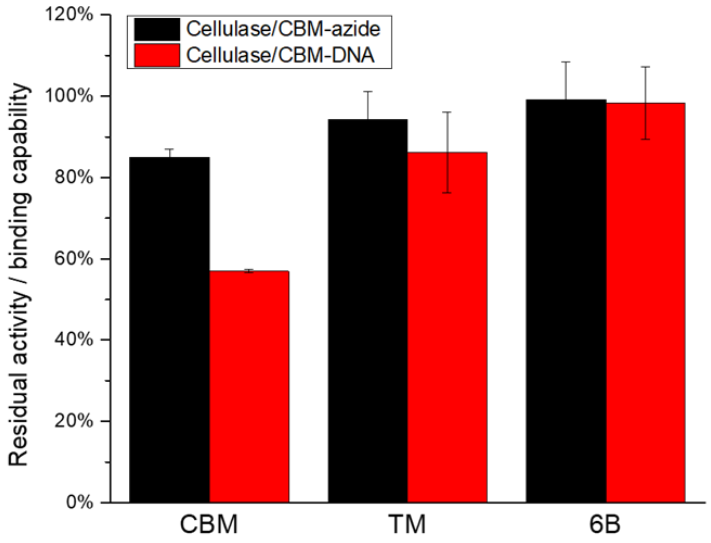


**Figure 4.5** Activity of cellulases and binding capability of CBM after modifications.

## Conclusion

Conjugation of cellulases /CBM with DNA linkers was successfully processed. The conjugation was proven by electrophoresis and indicated more than one DNA linker was assembled on all proteins. The activity and binding capability after modification was compared with native proteins and illustrated no significant changes in cellulase catalytic activity, but the binding capability was displayed according to DNA conjugation.

## References

1. Bayer, E. A.; Kenig, R.; Lamed, R., Adherence of Clostridium thermocellum to cellulose. *Journal of Bacteriology* **1983,** *156* (2), 818-827.

2. Lamed, R.; Setter, E.; Kenig, R.; Bayer, E. In *The cellulosome—a discrete cell surface organelle of Clostridium thermocellum which exhibits separate antigenic, cellulose-binding and various cellulolytic activities*, Biotechnol. Bioeng. Symp, 1983.

3. Bayer, E. A.; Chanzy, H.; Lamed, R.; Shoham, Y., Cellulose, cellulases and cellulosomes. *Current opinion in structural biology* **1998,** *8* (5), 548-557.

4. Shoham, Y.; Lamed, R.; Bayer, E. A., The cellulosome concept as an efficient microbial strategy for the degradation of insoluble polysaccharides. *Trends in microbiology* **1999,** *7* (7), 275-281.

5. Bayer, E. A.; Belaich, J.-P.; Shoham, Y.; Lamed, R., The cellulosomes: multienzyme machines for degradation of plant cell wall polysaccharides. *Annu. Rev. Microbiol.* **2004,** *58*, 521-554.

6. Doi, R. H.; Kosugi, A., Cellulosomes: plant-cell-wall-degrading enzyme complexes. *Nature reviews microbiology* **2004,** *2* (7), 541-551.

7. Boisset, C.; Chanzy, H.; Henrissat, B.; LAMED, R.; SHOHAM, Y.; BAYER, E. A., Digestion of crystalline cellulose substrates by the Clostridium thermocellum cellulosome: structural and morphological aspects. *Biochemical Journal* **1999,** *340* (3), 829-835.

8. Demain, A. L.; Newcomb, M.; Wu, J. D., Cellulase, clostridia, and ethanol. *Microbiol. Mol. Biol. Rev.* **2005,** *69* (1), 124-154.

9. Ng, T. K.; Zeikus, J., Comparison of extracellular cellulase activities of Clostridium thermocellum LQRI and Trichoderma reesei QM9414. *Appl. Environ. Microbiol.* **1981,** *42* (2), 231-240.

10. Fierobe, H.-P.; Bayer, E. A.; Tardif, C.; Czjzek, M.; Mechaly, A.; Bélaıch, A.; Lamed, R.; Shoham, Y.; Bélaıch, J.-P., Degradation of cellulose substrates by cellulosome chimeras Substrate targeting versus proximity of enzyme components. *Journal of Biological Chemistry* **2002,** *277* (51), 49621-49630.

11. Mori, Y.; Ozasa, S.; Kitaoka, M.; Noda, S.; Tanaka, T.; Ichinose, H.; Kamiya, N., Aligning an endoglucanase Cel5A from Thermobifida fusca on a DNA scaffold: potent design of an artificial cellulosome. *Chemical Communications* **2013,** *49* (62), 6971-6973.

12. Sun, Q.; Madan, B.; Tsai, S.-L.; DeLisa, M. P.; Chen, W., Creation of artificial cellulosomes on DNA scaffolds by zinc finger protein-guided assembly for efficient cellulose hydrolysis. *Chemical Communications* **2014,** *50* (12), 1423-1425.

13. Sun, Q.; Chen, W., HaloTag mediated artificial cellulosome assembly on a rolling circle amplification DNA template for efficient cellulose hydrolysis. *Chemical Communications* **2016,** *52* (40), 6701-6704.

14. Dziadek, S.; Jacques, S.; Bundle, D. R., A Novel Linker Methodology for the Synthesis of Tailored Conjugate Vaccines Composed of Complex Carbohydrate Antigens and Specific TH-Cell Peptide Epitopes. *Chemistry – A European Journal* **2008,** *14* (19), 5908-5917.

15. ZHAO, Y. R.; YANG, Q.; HUANG, Y.; GAI, S.; YE, H.; ZHAO, L.; YANG, C.; GUO, H.; ZHOU, X.; XIE, H.; ZHU, H.; XU, Y.; TONG, Q.; JIA, J.; CAO, M.; LI, W.; GAO, S.; GUO, Z.; BAI, L.; LI, C.; YANG, Y.; WANG, C.; YE, Z. Conjugation Linkers, Cell Binding Molecule-Drug Conjugates Containing the Likers, Methods of Making and Uses Such Conjugates with the Linkers. 2018.

16. Lee, K.; Kim, H.-J.; Kim, J., Design Principle of Conjugated Polyelectrolytes to Make Them Water-Soluble and Highly Emissive. *Advanced Functional Materials* **2012,** *22* (5), 1076-1086.

17. Xiao, Z.; Storms, R.; Tsang, A., Microplate‐based filter paper assay to measure total cellulase activity. *Biotechnology and Bioengineering* **2004,** *88* (7), 832-837.

# CHAPTER 5

# ESTABLISHING ARTIFICIAL CELLULOSOMES WITH DNA SCAFFOLDS

## Introduction

With the growing demand for energy in modern society, the extensive use of fossil fuels has raised the necessity for innovative and sustainable substitutes for petroleum[1, 2]. Biofuels, such as bioethanol, are proper alternatives, which can be produced from the fermentation of soluble sugars hydrolyzed from lignocellulosic biomass. Lignocellulose, consisting of cellulose, hemicellulose, and lignin, is the most abundant sustainable natural resource of carbohydrate polymers available for conversion to fuels. However, biofuel production has been limited by the hydrolysis of cellulosic biomass because of its recalcitrance to enzyme hydrolysis[3-5]. The recalcitrance is attributed to the interconnected units in lignocellulose, where lignin and carbohydrates (cellulose and hemicellulose) form lignin-carbohydrate complexes[6]. Besides, the high crystallinity and microfibrillar structure of cellulose is a barrier for enzymatic digestion of polysaccharides into fermentable sugars[7]. Current conversion processes mainly rely on thermo-chemical pretreatment and high enzyme loading, resulting in high manufacturing costs. Boosting catalytic activity of cellulases can be a potential solution to overcome the economic barriers to biomass conversion.

Cellulosomes are multienzyme complexes either attached to or secreted from cells. The high efficiency of cellulosomes in degrading has inspired scientists to develop artificial multienzyme complexes to reconstruct the natural structure. The flexibility of building artificial

cellulosomes should be more compatible with industrial applications and could help to investigate the mechanism of the cellulosome synergy effect.

Full sequencing of cellulosome from *Clostridium thermocellum* was reconstructed *in vitro*, and the reconstituted full-size cellulosome was 21% less active than natural cellulosome[8]. It is mainly because the mechanism of cellulosome hydrolysis is not fully discovered, such as the impact of sequence and spatial arrangement of cellulases and CBM.

Cellulosomes mediated by DNA were investigated leveraging the self-assemble property of DNA strands and convenience in producing controllable structures. Herein, we report a cellulosome design strategy for a various arrangement of enzymes and correlate the arrangements with cellulosome efficiency. Cellulases and CBM were first conjugated with single-stranded DNA linkers through "click" chemistry, followed by assembling onto pre-programmed DNA templates. Adjustment of DNA linkers attached will alter the position of each component in the complex.

**Experimental Section**

**Materials**. Same materials were used as described in chapter 4.

**Synthesis of cellulosomes with DNA scaffolds.** Synthesis of DNA labeled cellulases and CBM were described in chapter 4. One endo-cellulase, one exo-cellulase, and one CBM with different DNA linkers were annealed with DNA template A or B (Table 5.1) with a 1:1.5 molar ratio. The mixtures were heated at 65°C for 15min, followed by incubation in the water bath gradually cooled down to room temperature.

**Aggregation of cellulosomes**. Two cellulases and one CBM labeled with DNA linkers were first annealed to template C (Table 5.1) with a 1:1.5 molar ratio, as mentioned above. The

3-component cellulosome generated had a single-stranded DNA end, which was complementary to the aggregation DNAs. The aggregation DNA 2, 3, 4, 5 were then added into the mixtures with 1:2, 1:3, 1:4, and 1:5 molar ratio to the cellulosomes obtained and incubated overnight at room temperature to form complexes with 2, 3, 4, 5 of the 3-component cellulosomes respectively.

**Table 5.1** List of DNA sequences

| **DNA** | **Sequence** |
|---|---|
| Linker 1 | 5'-CCA ACC CAG TCA TGT GTG TTT /3DBCON/-3' |
| Linker 2 | 5'-TAG CAT CCT ACC TGT CCG TTT /3DBCON/-3' |
| Linker 3 | 5'-TAA GCT TGC GAG ACG TCT TTT /3DBCON/-3' |
| Template A | 5'-CAC ACA TGA CTG GGT TGG T CGG ACA GGT AGG ATG CTA T AGA CGT CTC GCA AGC TTA-3' |
| Template B | 5'-CAC ACA TGA CTG GGT TGG TTTTTTTTTT CGG ACA GGT AGG ATG CTA TTTTTTTTTT AGA CGT CTC GCA AGC TTA-3' |
| Template C | 5'-CAC ACA TGA CTG GGT TGG T CGG ACA GGT AGG ATG CTA T AGA CGT CTC GCA AGC TTA T GGT AAT GAA GGG CGG AGT-3' |
| Aggregation 2 | 5'-ACT CCG CCC TTC ATT ACC T ACT CCG CCC TTC ATT ACC-3' |
| Aggregation 3 | 5'-ACT CCG CCC TTC ATT ACC T ACT CCG CCC TTC ATT ACC T ACT CCG CCC TTC ATT ACC-3' |
| Aggregation 4 | 5'-ACT CCG CCC TTC ATT ACC T ACT CCG CCC TTC ATT ACC T ACT CCG CCC TTC ATT ACC T ACT CCG CCC TTC ATT ACC-3' |
| Aggregation 5 | 5'-ACT CCG CCC TTC ATT ACC T ACT CCG CCC TTC ATT ACC T ACT CCG CCC TTC ATT ACC T ACT CCG CCC TTC ATT ACC T ACT CCG CCC TTC ATT ACC-3' |

**Measurement of catalytic activity.** Activity of cellulosome and free enzyme mixtures were assayed with filter paper as described in chapter 4.

## Results and Discussion

**Activity of cellulosome complexes with different sequence and spatial arrangement.** Cellulosomes were first assembled with CBM, CelTM, and CBHII (CBHII-cellulosome). Complexes with 1 base spacing delivered similar but a slightly improved activity compared to the free enzyme mixture. The complex structures with different sequence arrangements demonstrated similar biocatalytic efficiencies (Figure 5.1). However, when proteins were assembled to template B with 10 base spacing, the structure with CBHII in the middle demonstrated about 1.5-fold enhancement in catalytic activity, while the complex with CelTM in the middle showed even a lower activity compared to the free enzyme mixture. Apparently, the distance between enzymes is important when more flexible structures with longer distances could result in the higher catalytic activity of the complex. The synergy effect of the cellulosomes was impacted by relative positions of the proteins where the placement of the exo-cellulase in the middle was the optimal organization for this enzyme combination.

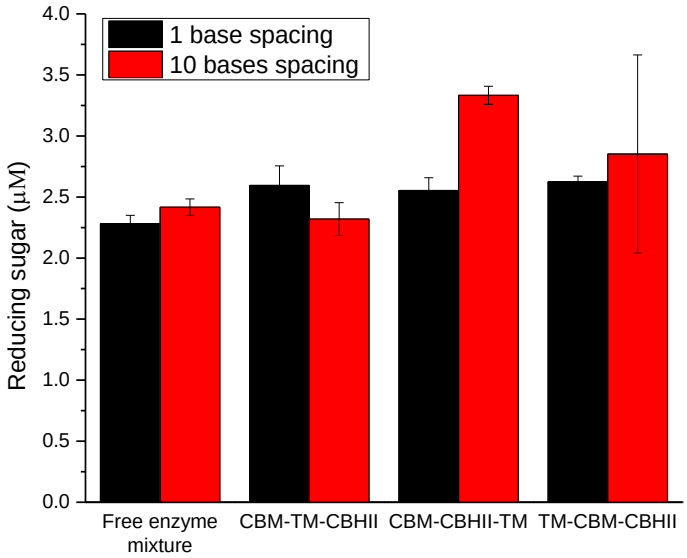


**Figure 5.1** Catalytic activity of CBHII-cellulosomes vs. free enzyme mixtures against filter paper.

**Variations of the complex size**. The first discovered natural cellulosome contains 9 catalytic domains, which demonstrated significant activity improvement attributed to the synergy effect among the enzymes [9, 10]. To illustrate the impact of cellulosome size, the assembled CBM-TM-CBHII complexes were aggregated to form structures with different amounts of enzymes. The activity tests demonstrated similar catalytic efficiency among different sizes of the aggregates, indicating the size of the complex did not affect the activity of CBM-TM-CBHII combinations (Figure 5.2).

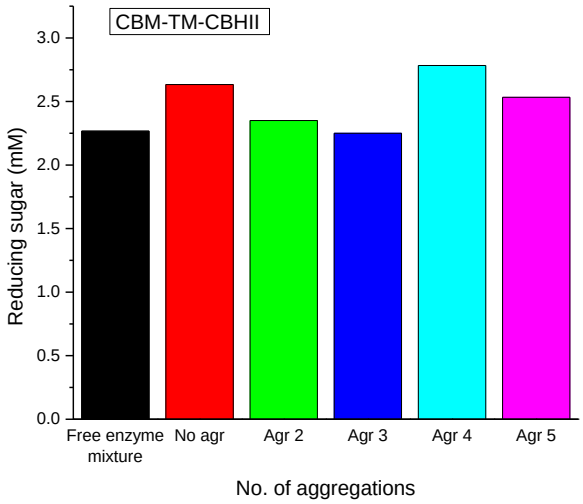


**Figure 5.2** Catalytic activity of CBM-TM-CBHII cellulosome aggregations. No agr represents the 3-component complex of CBM-TM-CBM. Agr 2, Agr 3, Agr 4, and Agr 5 are the aggregation of 2, 3, 4 and 5 CBM-TM-CBHII complexes separately.

**Variations of exo-cellulases**. Cellulosomes with Cel6B (Cel6B-cellulosomes) were designed to explore the synergy effect using an alternative exo-cellulase enzyme. A series of cellulosomes with different relative positions of Cel6B, CBM and TM proteins were generated using template A. All the assembled complexes demonstrated about 2-fold enhancement in catalytic activity compared to the free enzyme mixture (Figure 5.3). These cellulosomes showed

a significantly improved biocatalytic activity compared to CBHII-cellulosomes. The structures with different sequence arrangements of the proteins demonstrated similar biocatalytic activity, indicating the relative positions of proteins were not as significant as the synergy effect among enzymes.

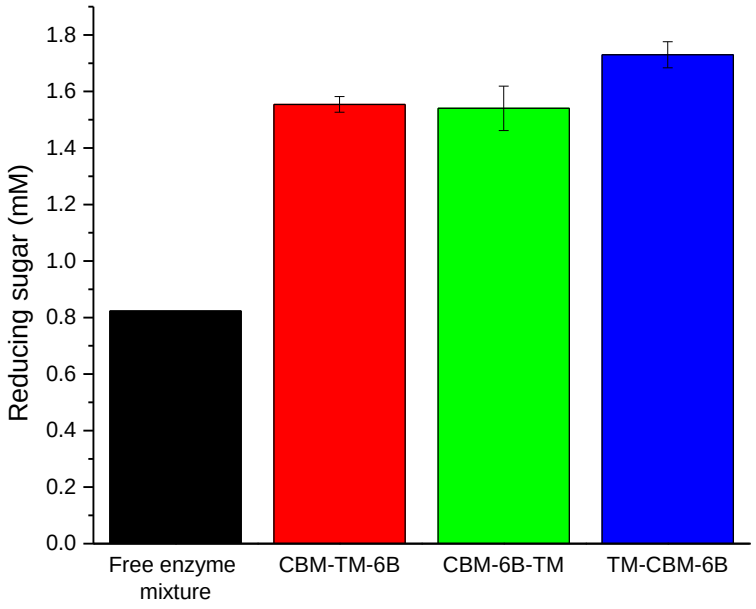


**Figure 5.3** Catalytic activity of Cel6B-cellulosomes vs. free enzyme mixtures.

## Conclusion

Cellulosomes based on DNA scaffolds had been generated to study the effect of the sequence and spatial arrangement of enzymes on catalytic activity of the multienzyme complexes. Cellulosomes with CBM, CelTM, and CBHII demonstrated similar activity to free enzyme mixtures when assembled with only 1 base spacer between proteins. When the distance between the proteins was increased to 10 bases, the effect of the protein specific locations was clearly observed. Placement of CBHII in the middle of the complex provided a 1.5-fold improvement of the biocatalytic activity, however, placing CelTM in the middle of the complex had slightly lowered catalytic activity compared to the free enzyme mixture. Aggregations of

CBM-TM-CBHII cellulosome to generate larger structured revealed no effect on the catalytic activity of the complexes. Cellulosomes designed with CBM, CelTM, and Cel6B demonstrated up to 2.2-fold activity improvement, confirming the synergy effect among the enzymes in the complex. In this complex, variations in protein sequence arrangements had little impact on catalytic efficiency of the complexes.

**References**


1. Ragauskas, A. J.; Williams, C. K.; Davison, B. H.; Britovsek, G.; Cairney, J.; Eckert, C. A.; Frederick, W. J.; Hallett, J. P.; Leak, D. J.; Liotta, C. L., The path forward for biofuels and biomaterials. *science* **2006,** *311* (5760), 484-489.

2. Hill, J.; Polasky, S.; Nelson, E.; Tilman, D.; Huo, H.; Ludwig, L.; Neumann, J.; Zheng, H.; Bonta, D., Climate change and health costs of air emissions from biofuels and gasoline. *Proceedings of the National Academy of Sciences* **2009,** *106* (6), 2077-2082.

3. Demain, A. L.; Newcomb, M.; Wu, J. D., Cellulase, clostridia, and ethanol. *Microbiol. Mol. Biol. Rev.* **2005,** *69* (1), 124-154.

4. Himmel, M. E.; Ding, S.-Y.; Johnson, D. K.; Adney, W. S.; Nimlos, M. R.; Brady, J. W.; Foust, T. D., Biomass recalcitrance: engineering plants and enzymes for biofuels production. *science* **2007,** *315* (5813), 804-807.

5. Artzi, L.; Morag, E.; Barak, Y.; Lamed, R.; Bayer, E. A., Clostridium clariflavum: key cellulosome players are revealed by proteomic analysis. *MBio* **2015,** *6* (3), e00411-15.

6. Pan, X.; Kadla, J. F.; Ehara, K.; Gilkes, N.; Saddler, J. N., Organosolv ethanol lignin from hybrid poplar as a radical scavenger: relationship between lignin structure, extraction

conditions, and antioxidant activity. *Journal of agricultural and food chemistry* **2006,** *54* (16), 5806-5813.

7. Yang, B.; Dai, Z.; Ding, S.-Y.; Wyman, C. E., Enzymatic hydrolysis of cellulosic biomass. *Biofuels* **2011,** *2* (4), 421-449.

8. Krauss, J.; Zverlov, V. V.; Schwarz, W. H., In vitro reconstitution of the complete Clostridium thermocellum cellulosome and synergistic activity on crystalline cellulose. *Appl. Environ. Microbiol.* **2012,** *78* (12), 4301-4307.

9. Bayer, E. A.; Kenig, R.; Lamed, R., Adherence of Clostridium thermocellum to cellulose. *Journal of Bacteriology* **1983,** *156* (2), 818-827.

10. Lamed, R.; Setter, E.; Kenig, R.; Bayer, E. In *The cellulosome—a discrete cell surface organelle of Clostridium thermocellum which exhibits separate antigenic, cellulose-binding and various cellulolytic activities*, Biotechnol. Bioeng. Symp, 1983.

# CHAPTER 6

# CONCLUSIONS AND FUTURE OUTLOOK

## Conclusions

In this dissertation, we have presented the establishment of enzyme complexes with polymer and DNA scaffolds to improve enzyme thermal stability and catalytic activity, which could make enzymes more compatible with industrial applications. In Chapter 1, a literature review of enzyme thermal stability mechanism and methods to improve stability was presented. Cellulosome enzyme complexes with synergy effect were introduced along with the various aspects of artificial cellulosomes' design.

Chapter 2 described the implantation of lysozyme in molecular brushes with grafting through method. Enzyme conjugates had demonstrated up to 9 times extension of lysozyme half-life at 90°C, and the thermal stability improvement was explained as a result of crowding effect from PEG side chains. The higher the molecular weight of PEG, the stiffer the molecular brush, and the better in stabilizing enzyme structures at high temperature.

In chapter 3, the mechanism of PEG crowding effects on lysozyme thermal stability was investigated under different PEG concentrations with different molecular weights. The results showed the stability effect depends on PEG concentration and molecular weight. The higher molecular weight PEG revealed a greater improvement of thermal stability when the effect increased with the PEG concentration reaching the saturation at the critical overlap concentrations of PEG. The observed thermal stabilization was confirmed with CD spectra by monitoring conformational changes of LYZ with temperature and with MD simulations. SAXS

and DLS experiments evidenced the role of PEG in preventing LYZ aggregation due to LYZ-PEG hydrophobic interactions at elevated temperatures.

Chapter 4 described methods to generate cellulases and CBM conjugates with DNA linkers, which can be used to establish artificial cellulosomes with specific sequence arrangement of proteins in the complex. Proteins were first modified with azido-$PEG_3$-NHS ester through lysine coupling, followed by SPAAC with DNA-DBCO to achieve the conjugation. The success of conjugation and purification was confirmed by.

Chapter 5 demonstrated the generation of artificial cellulosomes based on DNA scaffolds. DNA labeled cellulases/CBM were assembled onto preprogrammed DNA scaffolds to explore the potential of special arrangements of proteins in the complexes. The generated cellulosomes demonstrated up to 2.2-fold activity enhancement compared to the free enzyme mixture. It was revealed that the effect of flexibility and enzyme sequences on the complex biocatalytic activity is strongly dependent on activity of the individual enzymes used in the complex.

**Future work**

The dissertation outlines formation of polymer/DNA-enzyme complexes to improve enzyme thermal stability and catalytic activity, which can make enzyme combinations more compatible with industrial applications. The studied effects were revealed to be very specific for each studied enzyme. Investigation of the role of the enzyme structure and catalytic activity on properties of the complexes would be the next step toward an improved understanding of the complex design rules.

Another avenue for further progress is the development of computer models to accelerate the design of protein-polymer complexes. Our lab is in collaboration with a computer simulation lab to study the effects of enzyme sequence and spacing on cellulosome catalytic activity.

**Final Remarks**

Enzymes are highly valuable natural catalysts for industrial applications because of their high activity and specificity. However, a relatively narrow range of temperature tolerance and high costs are barriers in many applications. Design of enzyme-polymer complexes and conjugates with specific enzyme sequences and spatial arrangement demonstrated a potential for improvement of the catalytic performance and thermal stability of enzymes for efficient applications.

# APPENDIX A

## ENZYME CATALYTIC ACTIVITY AND THERMAL STABILITY

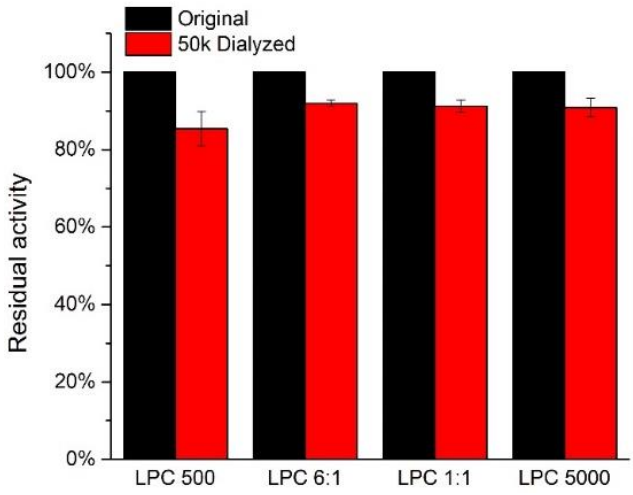


**Figure A1.** Lysozyme activity of LPC 500, LPC 6:1 and LPC 5000 for original solution (black bars) and in filtrate after 50k dialysis (red bars) of the polymerization mixture.

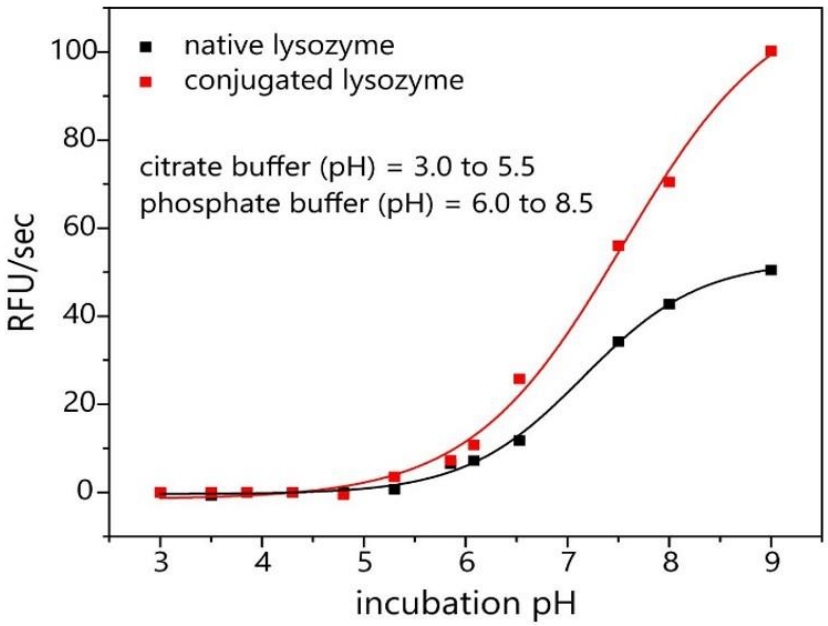


**Figure A2.** Effect of pH change on LYZ (black) and LPC (red) catalytic activity

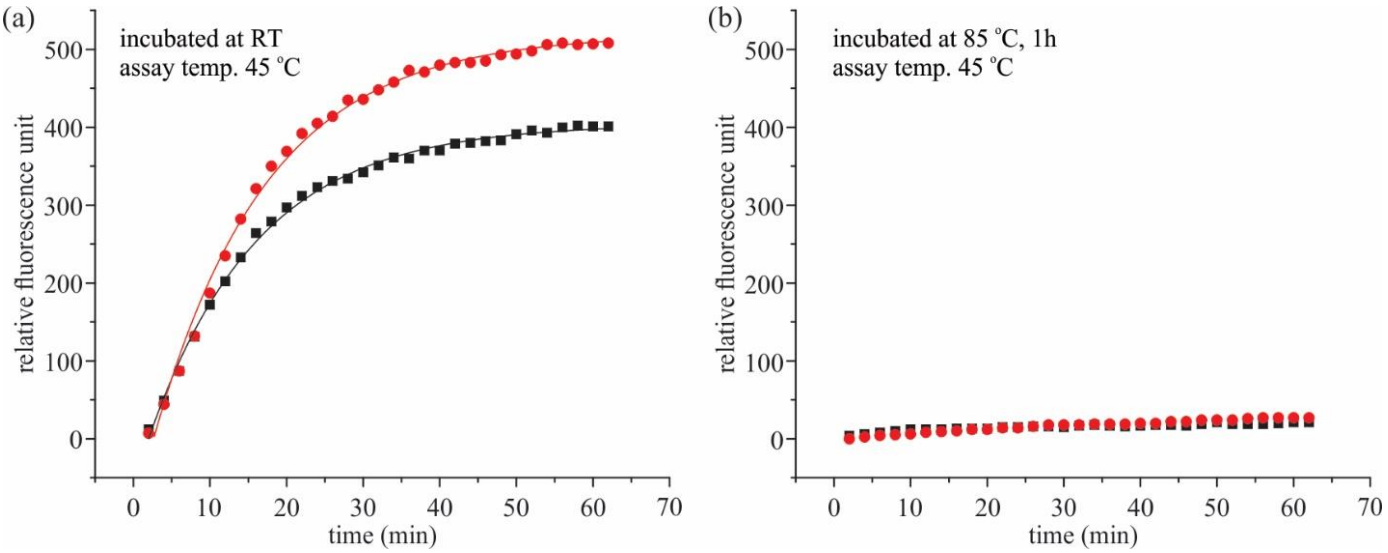


**Figure A2.** Thermal stability of LYZ added with only POEGMA. Comparison of the activity kinetic of LYZ-POEGMA (●) and native LYZ (■) preincubated at a) room temperature and b) at 85°C for 1h.

APPENDIX B

CHARACTERIZATION OF MOLECULAR BRUSHES

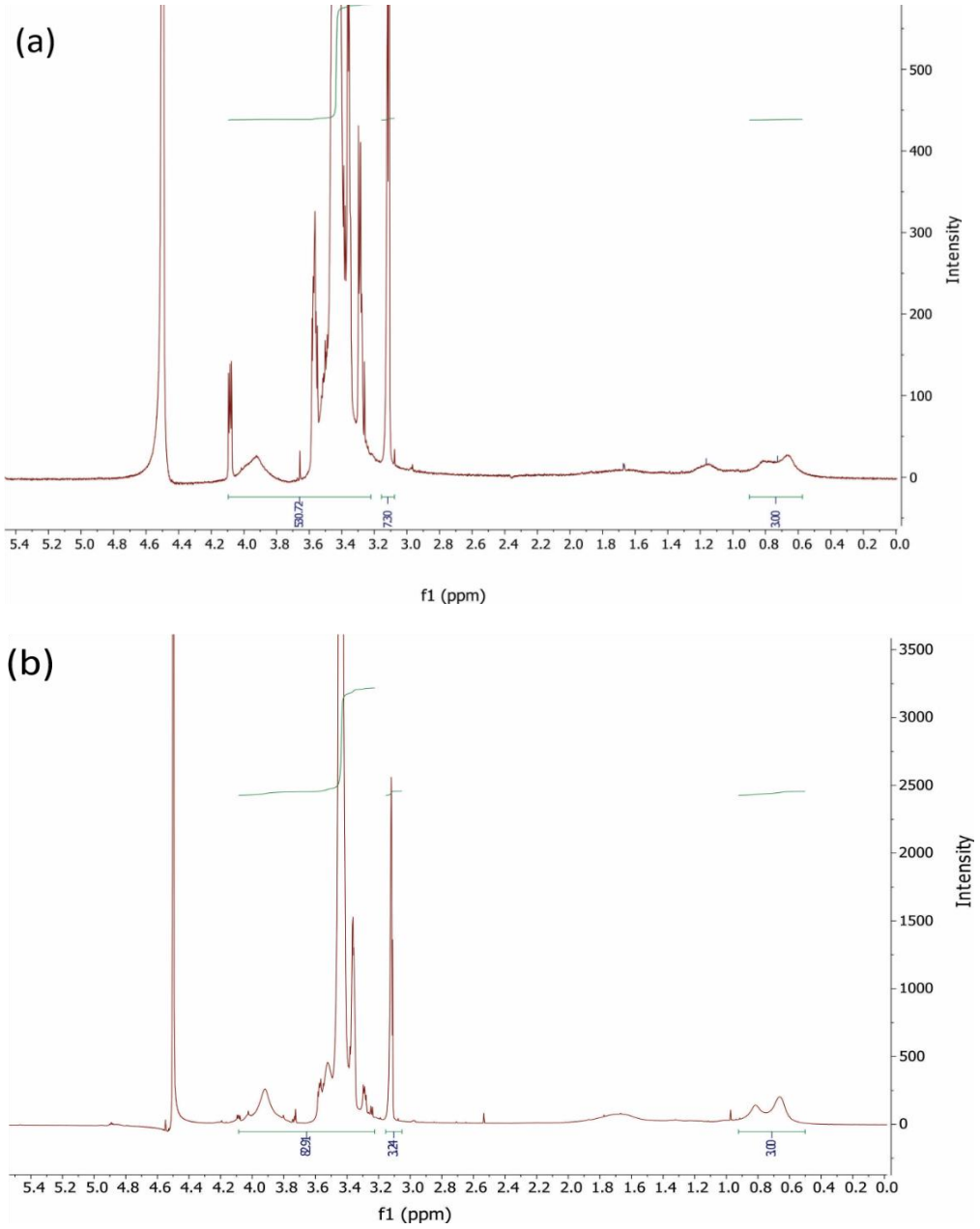


**Figure B1.** NMR spectra for (a) copolymer 1:1 and (b) copolymer 6:1.

**Table B1**. Molecular characteristics of the molecular brushes in θ-solvent

| Sample | $N_{SC}$ | $h$, nm | $N_{SC}^{1/2}l$, nm | $R_{SC,}$ nm | $F(h)/k_BT$ |
|---|---|---|---|---|---|
| LPC 500 | 8.95 | 0.25 | 1.04 | 1.7 | 2.74 |
| LPC 5000 | 111.5 | 0.25 | 3.68 | 9.2 | 6.36 |

**Table B2**. Molecular characteristics of the molecular brushes in melt

| Sample | $N_{bb}$ | $N_{SC}$ | $z^*$ | $z^{**}$ | $R$, nm | $R_{SC,}$ | $b$, nm | $l$, nm | $v$, nm$^3$ | z |
|---|---|---|---|---|---|---|---|---|---|---|
| LPC 500 | 87 | 8.95 | 0.6 | 1.4 | 12 | 1.56 | 0.63 | 0.38 | 0.065 | 1 |
| LPC 5000 | 15 | 111.5 | 0.17 | 1.4 | 9.4 | 5.16 | | | | |

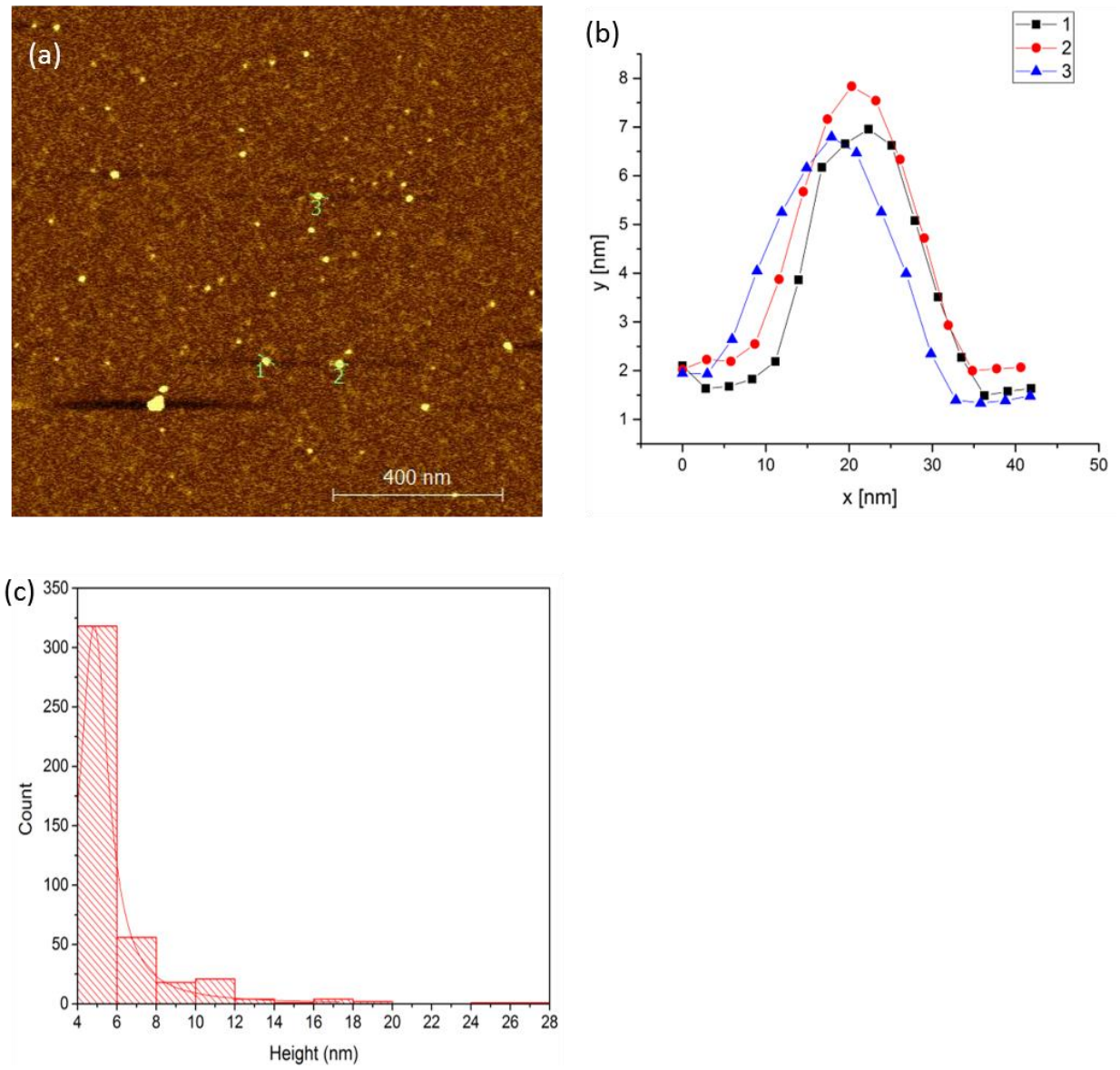


**Figure B2**. Representative SPM topography image (a) and cross-sectional profiles (b) of LPC 1:1 molecules (as labeled 1,2 and 3 on the SPM image), and height distribution (c). The average diameter is 4.85±0.89 nm.